

UC San Diego

UC San Diego Electronic Theses and Dissertations

Title

The Design and Investigation of a Passive Electricidal Urinary Catheter Surface

Permalink

<https://escholarship.org/uc/item/22g780fz>

Author

Gotlib, Oren

Publication Date

2019

Peer reviewed|Thesis/dissertation

UNIVERSITY OF CALIFORNIA SAN DIEGO

The Design and Investigation of a Passive Electricidal Urinary Catheter Coating

A Thesis submitted in partial satisfaction of the requirements
for the degree of Master of Science

in

Materials Science and Engineering

by

Oren Gotlib

Committee in charge:

Frank E. Talke, Chair
Marc A. Meyers
Frederick E. Spada
Michael T. Tolley

2019

Copyright
Oren Gotlib, 2019
All Rights Reserved

The Thesis of Oren Gotlib is approved, and it is acceptable in quality and form for publication on microfilm and electronically:

Chair

University of California San Diego

2019

DEDICATION

I would like to dedicate this thesis to my parents for giving me their full support and love. They are the foundation of my success; without them I would not be who I am today. I also dedicate this work to my loving wife, Jeannette, who was not only instrumental in my pursuit of a master's degree, but who has also been by my side these last twelve years, encouraging and motivating me each step of the way.

EPIGRAPH

“You’re on your own,
and you know what you know.
And YOU are the guy who’ll decide where to go.”
-Dr. Seuss Geisel

“A man should look for what is, and not for what he thinks should be.”
-Albert Einstein

“Do not fear failure.”
-Fortune Cookie, courtesy of Dr. Fred Spada

“If an expert says it can't be done, get another expert.”
-David Ben-Gurion

“Don’t find the fault, find the remedy”
-Henry Ford

“Innovation distinguishes between a leader and a follower”
-Steve Jobs

“All progress occurs because people want to be different.”
-Fortune Cookie, courtesy of Dr. Fred Spada

“When you reach the end of your rope, tie a knot in it and hang on.”
-Franklin D. Roosevelt

“It is during our darkest moments that we must focus to see the light.”
-Aristotle

“All religions, arts and sciences are branches of the same tree.”
-Albert Einstein

TABLE OF CONTENTS

Signature Page.....	iii
Dedication.....	iv
Epigraph.....	v
Table of Contents.....	vi
List of Figures.....	viii
List of Tables.....	x
Acknowledgements.....	xi
Vita.....	xii
Abstract of the Thesis.....	xiii
Chapter 1: Introduction to CAUTI and Methods of Prevention	1
1.1: Introduction.....	1
1.2: Catheter Associated Urinary Tract Infection.....	3
1.3: Biofilm Formation.....	5
1.4: Methods to Prevent Biofilm on Surfaces.....	7
Chapter 2: Selection of Active Materials and Rationale.....	18
Chapter 3: Catheter Coating Formulation and Coating Methods.....	27
3.1: Materials Used for Fabricating Urinary Catheters.....	27
3.2: Methods to Incorporate Active Materials into a Catheter Coating.....	30
3.3: Preparation of Coatings and Thin Film Samples	33
3.4: Fabrication of Coated Catheter Prototypes.....	35
Chapter 4: Experimental Methods.....	38
Chapter 5: Experimental Results.....	42
5.1: Open Circuit Cell Potential Measurements.....	42
5.2: Hydrogen Peroxide and pH Measurements.....	43
5.3: Microscopy of a Zn/Ag ₂ O:PDMS Composite Film.....	44

5.4: Goniometry.....	45
5.5: Antimicrobial Resistance Measurements.....	46
Chapter 6: Discussion of Experimental Results	53
Chapter 7: Conclusion.....	56
References.....	58

LIST OF FIGURES

Figure 1: A commercial silver coated Foley urinary catheter with inflated balloon (left). A representation of a Foley urinary catheter deployed in a female (right).....	3
Figure 2: Diagram showing a typical bacterium and surface organelles (A), the interactions between the bacterium and the substrate (B), and surface sensing mechanisms (C) [13].....	5
Figure 3: An illustration depicting planktonic bacteria in solution approaching the surface (A), adhering and colonizing the surface (B), excreting the protective EPS layer such that they form biofilms (C), and forming complex three-dimensional biofilm communities within hours (D)	6
Figure 4: A diagram showing the setup for an antimicrobial electrical current experiment in a catheter model. An ionic media inoculated with bacteria is sealed in a catheter section with two endcaps and exposed to electrode potentials from a DC power source [7]	11
Figure 5: A photo of an electroceutical, wound therapy bandage. A flap is pulled back to reveal the central cathode on the wound viewing window which is connected in series to the outer anode [31].....	12
Figure 6: Photos of Zn/Ag bioelectric wound dressing (top) composed of zinc electrodes 1mm OD (grey) and silver electrodes 2mm OD with a 5mm lattice parameter (bottom).	15
Figure 7: Pourbaix diagram for zinc in aqueous solution [37]	21
Figure 8: The Pourbaix diagram for silver in aqueous solution [37]	21
Figure 9: Superimposed Pourbaix diagrams of zinc (blue) and silver (red). At a pH of seven the potential of the overall reaction is +1.6 volts.....	22
Figure 10: A series of kinetic steps limiting the overall electrode reaction rate.....	25
Figure 11: An illustration of the degree of surface wettability based on the contact angle formed between a liquid drop and the solid surface	27
Figure 12: A depiction of how a primer is used to bond materials that have trouble physically bonding.31	
Figure 13: A schematic showing one method to imbed metal electrodes in the surface of PDMS. A combination of soft and photo lithography	32
Figure 14: A schematic revealing the process of fabricating AM:PDMS thin films. PDMS is measured onto a glass pane (A), AM is measured on weigh paper and poured over PDMS and mixed (B), a PETG mask is applied (C), the sample is spread across the well (D), the mask is removed and the glass pane is placed in an oven to cure (E), the film is removed with a straight razor	34
Figure 15: A photo showing composite films (left to right, top to bottom) Zn, Ag, Ag ₂ O, Ag-coated catheter, Ag/Ag ₂ O, Zn/Ag ₂ O mixed , Zn/Ag ₂ O striped, and a bio electric dressing	35
Figure 16: A schematic revealing the use of a mold to maintain AM at the surface of the catheter.	36

Figure 17: A simple machined aluminum mold and two steel lumen-molds 37

Figure 18: Photo displaying the final (balloon-free) single lumen Ag/Ag₂O:PDMS catheter (left) and a section of commercially available coated in Zn/Ag₂O:PDMS (right) 37

Figure 19: A plot of potential difference with respect to time. The potentials of silver foil relative to zinc foil in Air saturated synthetic urine and DI water are similar 42

Figure 20: Shows the concentration of hydrogen peroxide measured with respect to time (top-left) using either test scale (top-right). The synthetic urine increased alkalinity for samples containing zinc or silver oxide after a period of 13 days (bottom) 43

Figure 21: A Zn/Ag₂O:PDMS composite before and after (right and left, respectively) being exposed to urine following twenty-four hours in synthetic urine. A white crystal residue formed on the surface (A, B). Beneath the residue a brown discoloration is visible (C, D) 45

Figure 22: A bar chart showing contact angles measured for AM:PDMS composites accompanied by images of the contact angle formed on a PDMS (A) and Zn/Ag₂O:PDMS film (B). 46

Figure 23: A plot of absorbance OD₆₀₀ with respect to time for selected samples (left). A photo of a pure PDMS and Ag₂O:PDMS samples in inoculated synthetic urine (right). The more bacteria in solution the higher the absorbance 47

Figure 24: A plot of biofilm concentration in CFU/mL growing on the surface of selected samples following 48 hours. Samples with higher concentrations perform worse in inhibiting biofilm 48

Figure 25: A plot of absorbance OD₆₀₀ with respect to time for selected samples over a 6-day period 49

Figure 26: A plot of biofilm concentration in CFU/mL growing on the surface of selected samples following six days. Samples with higher concentrations perform worse in inhibiting biofilm 50

Figure 27: Zone of inhibited bacteria about the 8mm disk of AM:PDMS films on LB agar plates coated with E. coli (n=3). Radius of zone is measured from center of disk 51

Figure 28: Biofilm concentrations measured from catheter sections coated with antimicrobial composites following six days (n=5). Samples with higher concentrations perform worse in inhibiting biofilm. 52

LIST OF TABLES

Table 1: A list of pathogenic microorganisms associated with CAUTI [3].	4
Table 2: Shows five well known mechanisms to kill bacteria and the materials used to do so [3]	8
Table 3: A table showing minerals used in the human body. Some minerals are more essential than others and some are used in trace by coexisting microorganisms[33].	14
Table 4: List of half-reactions selected from the electrochemical series relevant to using the zinc-silver redox couple as a surface coating in an aqueous solution [42]. The standard reduction potentials are relative to the standard hydrogen electrode, at room temperature and unit activity.	19
Table 5: A table of polymers used to make medical devices. Polymers PVC, Silicone, TPU, PEEK, have been used to make catheters [47]	28
Table 6: Check boxes represent the following combinations of active materials that were studied.	34
Table 7: A simple recipe for the growth of urinary pathogens [61].	38

ACKNOWLEDGMENTS

I would like to acknowledge Professor Frank E. Talke, who guided me through this wonderful learning experience and who always had faith in my abilities. I remember meeting him for the first time following a seminar where he presented his ongoing research and pivot to solve medical problems. I was truly inspired by his ability to take problem solving of one field and apply it directly into another. At that moment, I could not help but insist that I attend one of his lab meetings, and without a second thought, he introduced me to his graduate students. Not only did Professor Talke offer me a chance to contribute to his research, but he also gave me a chance to solve a serious medical problem that for years I have taken very seriously. Such an opportunity is rare. After every iteration of my work, Professor Talke made sure to understand the progress and contributed positively to any gaps or walls. Although our work together has faced many challenges, he has given me the inspiration to see them as opportunities to learn and grow. He pushed me as hard as he could, and now I can see my true potential. As they say, “Anfangen ist leicht, beharren eine Kunst.” I can say without a doubt that working for Professor Frank Talke has been the greatest learning experience in my life and I am forever indebted to him.

I would like to acknowledge Professor Milton Saier and Andrew Bodnar, who reignited the ability to perform antimicrobial resistance testing. I would like to thank Professor Ping Liu and his students Matthew Gonzalez and Victoria Petrova for allowing me to use their lab. I would like to acknowledge Professor Tolley, Dr. Spada, and Dr. Alagiri, who invested in me and helped me grow as a scientist. Furthermore, I must thank Karcher Morris for being such an excellent mentor; his guidance was instrumental in the pursuit of my thesis. Finally, I would like to acknowledge Rafaela S. Torigoe and Simonas Vaitkus who have been working under me; these two undergraduate students have contributed above and beyond what was expected.

VITA

- 2014-2015 Undergraduate Research Assistant, University of California at Davis
- 2015 Bachelor of Science, University of California at Davis
- 2015-2017 Contractor Research Associate for U.S. Air Force, Ke’aki Technologies LLC
- 2018-2019 Graduate Research Assistant, University of California San Diego
- 2019 Master of Science, University of California San Diego

PUBLICATIONS

Gotlib O., Morris K., Spada F.E., Alagiri M., Patras K., and Talke, F.E. "Investigation of Zinc-Silver Oxide-Thermoplastic Composite for Application in a Biofilm Retardant Urinary Catheter." Proceedings of the ASME 2019 28th Conference on Information Storage and Processing Systems. ASME 2019 28th Conference on Information Storage and Processing Systems. San Diego, California, USA. June 27–28, 2019. V001T07A004. ASME. <https://doi.org/10.1115/ISPS2019-7517>

Johnson M.A., Davidson A.J., Russo R.M., Ferencz S.E., **Gotlib O.**, Rasmussen T.E., Neff L.P., Williams T.K. "Small changes, big effects: The hemodynamics of partial and complete aortic occlusion to inform next generation resuscitation techniques and technologies". J Trauma Acute Care Surg. 2017 Jun;82(6):1106-1111. doi: 10.1097/TA.0000000000001446. PMID: 28338590.

Keller B. A., Salcedo E. S., Williams T. K., Neff L. P., Carden A. J., Li Y., **Gotlib O.**, Tran N.K., Galante, J. M. "Design of a cost effective, hemodynamically adjustable model for resuscitative endovascular balloon occlusion of the aorta (REBOA) simulation". Journal of Trauma and Acute Care Surgery. 2016 Sep; 81(3):606-11. <http://doi.org/10.1097/TA.0000000000001153>

PRESENTATIONS

Alagiri M., **Gotlib O.**, Minori A.F., Patras K., Spada F.E., Tolley, M.T., Talke F.E. Investigation of Zinc – Silver Oxide –Thermoplastic composite for Application in a Biofilm Retardant Urinary Catheter, Information Storage and Processing Systems. University of California, San Diego. June 27, 2019

ABSTRACT OF THE THESIS

The Design and Investigation of a Passive Electricidal Urinary Catheter Coating

by

Oren Gotlib

Master of Science in Materials Science and Engineering

University of California San Diego, 2019

Professor Frank E. Talke, Chair

Catheter associated urinary tract infection (CAUTI) is a significant problem. Interdisciplinary teams have coordinated to address this problem, yet there is still a need for an adequate solution. Indwelling urinary catheters are at the root of prevalence of CAUTI. Urinary catheters with surfaces that are defenseless against the growth of infectious microorganisms, such as bacteria, are a risk to patients with urinary incontinence. This Master's thesis describes the design and investigation of a passive electricidal urinary catheter surface. This entails a discussion of methods to prevent CAUTI with catheter coatings, in addition to methods used to formulate and adhere coatings. The design of composite coatings using polydimethyl siloxane (PDMS), with active materials zinc, silver, and/or silver oxide powders is disclosed, thereafter. These coatings are designed so that the active materials are well adhered and allowed to react in the presence of bodily fluids. The oxidation reduction reactions that occur between the dissimilar metals in solution has the capability to create an environment at the catheter surface that includes electric fields, microcurrents, changes in pH, and generation of heavy metal ions and hydrogen peroxide. This environment is similar to

that of a zinc-silver galvanic cell, and has been found to alter the adhesion and proliferation of bacteria on surfaces and their ability to form dangerous biofilms. The composite coatings made in the lab were tested to determine their reactivity and biocidal effects. Methods used to quantify the generation of hydrogen peroxide, electric potentials, changes in pH, and inhibition of planktonic bacteria and biofilm in synthetic urine are discussed. The results of these tests show that the coatings are able to generate potentials and hydrogen peroxide in synthetic urine. Coatings containing combinations of zinc and silver oxide or silver and silver oxide have the greatest antimicrobial effects compared to controls. These coatings also inhibited biofilm as good as, if not better than, commercially available antimicrobial specimens.

Chapter 1: Introduction to CAUTI and Methods of Prevention

1.1 Introduction

The Center for Disease Control and Prevention and the Department of Health and Human Resources [1] reported that urinary tract infections (UTIs) are the most common type of healthcare-associated infection reported to the National Healthcare Safety Network. In fact, UTIs acquired in hospitals are 75% associated with urinary catheters. A urinary catheter is intended to collect urine from a patient with urinary incontinence. Approximately 15-25% of hospitalized patients receive urinary catheters during a regular hospital stay. It is estimated that hospitals spend over \$1 billion in managing catheter associated urinary tract infections or CAUTI [2]. Infection is most often associated with endogenous bacteria that colonize the surfaces of the urinary catheter, and form biofilms inside the patients [1]. For decades, the medical community has been trying to develop improved antifouling and biocidal materials that can be deposited onto the surfaces of medical devices [1-21]. The ability to maintain the sterility of a surface against the resistant nature of virulent bacteria would prevent thousands of patients from contracting life-threatening infections.

One solution for reducing the number of infections associated with catheters is a surface coating or treatment that either reduces the attachment of microorganisms to the surface or kills microorganisms on or near the surface. Biocidal surface treatments and coatings for catheters that have been specifically designed to kill microorganisms are popular. Coatings that contain toxic molecules like silver, copper, and various antibiotics and proteins have been developed, but lack clinical efficacy [3], [6], [14], [22]. Additionally, antifouling surface treatments and coatings for catheters have been developed to specifically resist attachment of microorganisms. Developers have used reactive ion etching to create micron-sized surface topology that reduces colonization of bacteria [23], [24]. There are also hydrophilic coatings for catheters that are shown to reduce the concentration of biofilm on surfaces [3], [8], [25]. Many of these antifouling surfaces are still being investigated and have not become a standard for urinary catheters.

Studies have shown that electrical fields and currents have the potential to reduce biofilm. As far back as 1974, antibacterial effects were observed using weak direct current between silver electrodes. In 2009, anti-biofilm effects were observed on Staphylococcus and Pseudomonas bacteria strains following sustained exposure to low-intensity electrical current; this effect was given the name electricide [16]. For reasons directly associated with CAUTI, the electricidal effect was also applied in a catheter model [17]. Developers of a biofilm-inhibiting wound dressing aimed to create low-intensity electrical current by using galvanic materials exposed to bodily fluids, instead of using wiring or a power supply [18], [19]. A wireless electricidal surface is advantageous because it is simpler to use and contains less components, but the design has yet to be achieved on urinary catheters.

This master's thesis aims to investigate and design a surface coating for urinary catheters that is able to generate passive electricidal effects following exposure to bodily fluids. First discussed is how bacteria cause CAUTI. Next, techniques that have been developed by others to mitigate bacterial growth on catheters are described. Thereafter, the author's methods are presented to produce a passive, electricidal coating for urinary catheters. Finally, a presentation and discussion of the experimental results will be given related to the performance of the coating.

1.2 Catheter Associated Urinary Tract Infection

The Center for Disease Control and Prevention (CDC) reports that the most important risk factor for developing catheter associated urinary tract infections (CAUTI) is prolonged use of a urinary catheter [1]. Figure 1 shows an image of a silver coated Foley urinary catheter used for urinary incontinence (left) and an anatomical chart with a urinary catheter deployed into the urinary tract, secured in the bladder with an inflated distal balloon (right). Health care professionals must also perform consistent aseptic handling when first deploying the catheter, and when flushing and sampling from the urine collection bag, until the time at which the catheter can be removed. Even when health care professionals actively perform safe and sterile urinary catheter protocols, ambient microorganisms can migrate along the surface of urinary catheters and their components. A list of microorganisms most commonly associated with CAUTI is shown in Table 1 [3]. These microorganisms can be categorized into gram-negative bacteria, gram-positive bacteria, and fungi. After a period of 72 hours, bacteria often enter and colonize the urinary tract. For this reason, prolonged use of a urinary catheter creates the highest risk of infection. Hospitals spend millions of dollars each year on treating patients with CAUTI, and on fines relating to infection control [2]. Numerous efforts have been made to understand and eliminate CAUTI.

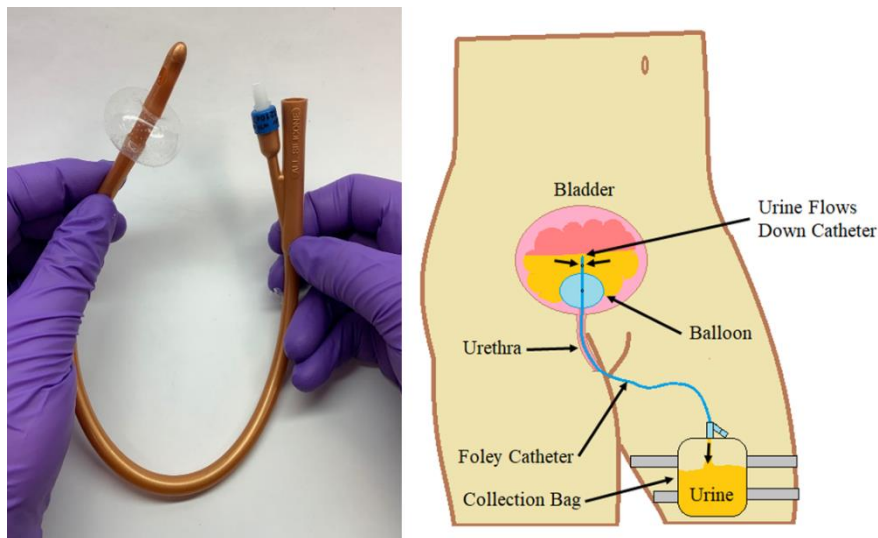


Figure 1: A commercial silver coated Foley urinary catheter with inflated balloon (left). A representation of a Foley urinary catheter deployed in a female (right)

Table 1: A list of pathogenic microorganisms associated with CAUTI [3].
 *Most clinically relevant/virulent species with respect to UTIs [26]

Microorganism Name	Type
Bacillus subtilis	Gram Positive Bacteria
Enterococcus faecalis	Gram Positive Bacteria
Enterococcus faecium	Gram Positive Bacteria
Staphylococcus aureus*	Gram Positive Bacteria
Staphylococcus epidermidis*	Gram Positive Bacteria
Escherichia coli*	Gram Negative Bacteria
Klebsiella pneumonia*	Gram Negative Bacteria
Morganella morganii*	Gram Negative Bacteria
Proteus mirabilis*	Gram Negative Bacteria
Providencia spp.	Gram Negative Bacteria
Pseudomonas aeruginosa*	Gram Negative Bacteria
Candida glabrata	Fungi
Candida tropicalis	Fungi
Candida albicans*	Fungi

Implants are often associated with infection, as they provide an excellent surface for bacterial colonization. Bacteria are present everywhere in nature and have many strategies to communicate and invade humans. Bacterial adhesion is highly dependent on the physical properties of the media, the surface, and the bacteria membrane. Interactions between bacteria and solid surfaces are visualized in Figure 2 [27]. Extracellular organelles (Figure 2A) operate to create physical attachments of the cell body to a surface. To adhere to a surface, the bacteria must engage in any number of interactions associated with the surface, e.g., van der Waals forces, hydrophobic interactions, steric forces, and the presence of small molecules (Figure 2B), by using methods that sense surface concentrations of pH and osmolytes (Figure 2C).

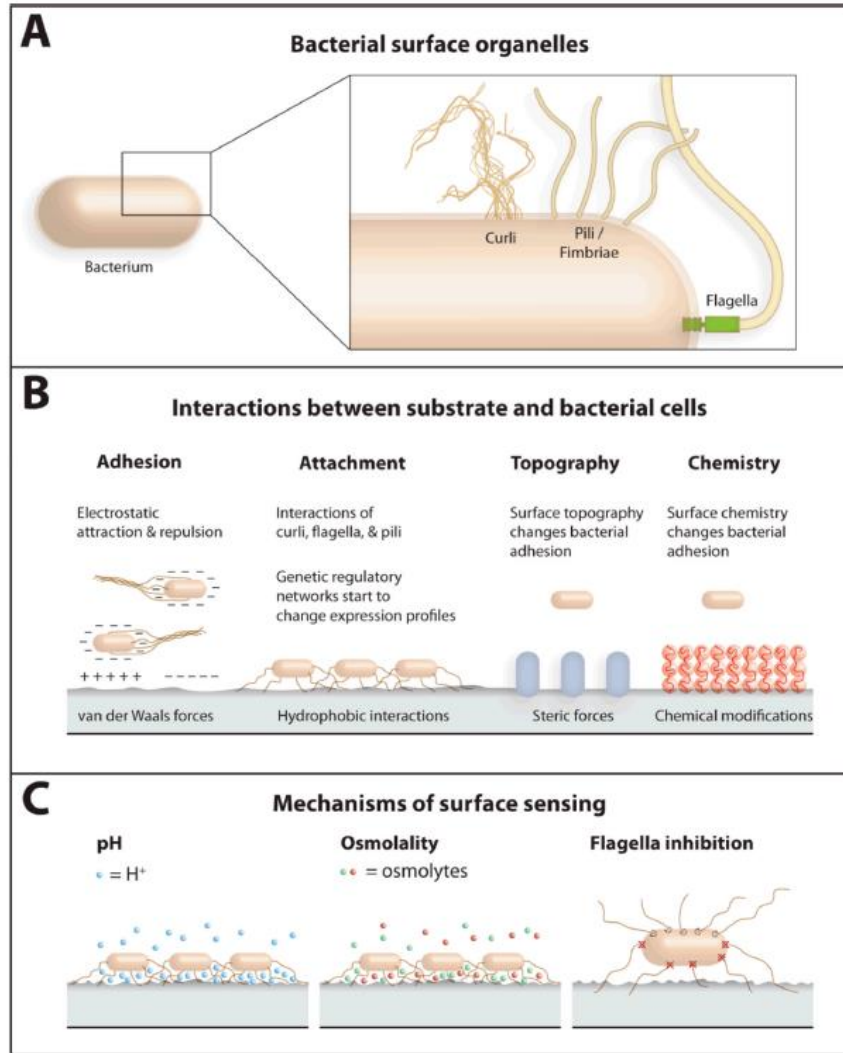


Figure 2: Diagram showing a typical bacterium and surface organelles (A), the interactions between the bacterium and the substrate (B), and surface sensing mechanisms (C) [13]

1.3 Biofilm Formation

Upon contacting a surface, cell attachment occurs in two phases. The initial phase is regarded as a short-term, reversible physiochemical phenomenon, where water is lost at the interfacial layer, surface molecules change structurally, and the cell repositions its body to maximize contact with the surface. The secondary phase is comprised of an irreversible long-term van der Waals phenomenon and the secretion of various proteins that anchor the cell body to the surface [27]. The net surface charge of most bacteria is negative, which is why they prefer to interact with surfaces that are positively charged [28]. Attachment

of bacteria to surfaces improves antibiotic resistance by reducing the net negative surface charge of bacterial cells and enhancing the stability of the membrane. The effect can disappear in media with high concentrations of ions due the ability of bacteria to screen the surface using ions from the solution [27], [28]. In other words, bacteria have the ability to attach to surfaces that initially prevent attachment by depositing a layer of environmental and innate proteins or ions that condition the surface and nullify functional groups that would normally reduce adhesion. [27]. Bacteria prefer adhering to hydrophilic materials (materials with large surface energy) under the condition that the surface energy of the bacterium is greater than the surface energy of the liquid they are suspended in. However, bacteria have smaller surface energy than that of the liquid in which they suspend, i.e., cells often attach to materials with a hydrophobic surface (materials with lower surface energy) [3], [14], [27], [28].

During an acute infection, bacteria promptly proliferate and spread across a surface as unicellular organisms. However, during chronic infection, bacteria typically colonize the surfaces of implants and/or tissues as multicellular aggregates, termed biofilms [14]. The latter process, illustrated in Figure 3, shows how free flowing/moving (planktonic) bacteria in a solution (A), adhere to and colonize a surface of interest (B), initiate genetic expression of new physical characteristics/traits (C), and change into biofilms (3D).

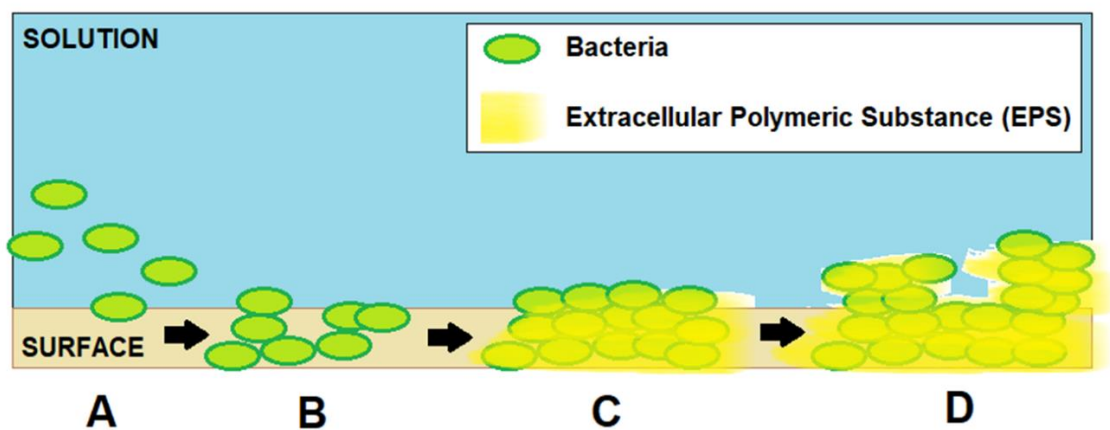


Figure 3: An illustration depicting planktonic bacteria in solution approaching the surface (A), adhering and colonizing the surface (B), excreting the protective EPS layer such that they form biofilms (C), and forming complex three-dimensional biofilm communities within hours (D)

Biofilms are aggregates of bacteria that communicate and maintain robust proliferation by encompassing themselves in self-secreted networks of extracellular polymeric substance (EPS) [3], [28]. This matrix-like network allows a bacterial colony to respond to environmental stress that would normally inhibit proliferation. Stresses include, but are not limited to, external attack, physical conditions, and nutrient limitation [27]. For example, EPS secretion can act as a physical barrier against mechanical damage and shear stress caused by fluid flow. The EPS assists bacterial colonies in many ways that include improved adhesion, communication, and nutrient supply [28].

In the 3D biofilm matrix, colonies found at the surfaces are metabolically active, while the innermost colonies survive as non-growing, dormant colonies, well protected by the matrix and very difficult to eradicate; these well protected bacteria are also known as “persisters” [14]. Compared to planktonic cells freely suspended in fluids, bacteria existing in the biofilm can carry out robust levels of lateral gene transfers. This is relevant because the persister cells are not only able to resist antibiotics, but they are able to effectively share relevant genes that have helped them survive [27], [28]. Traditionally, control of infection typically begins with removal of the implant or foreign body followed by a variety of antibiotics and anticoagulants [14], [26].

To be clear, biofilms exhibit resistance to antibiotic treatment via the following mechanisms: physical barrier of the biofilm matrix, the presence of dormant persister cells, exceedingly resistant small colony mutants, and an increase in the regulation of biofilm specific antibiotic resistance genes. Thus, planktonic bacteria are 10-100 times less resistant to antimicrobials than biofilms [29], which sheds light to why CAUTIs are difficult to eliminate with traditional antibiotic regimens. For this reason, the biomedical engineering community has been trying to develop improved antifouling and biocidal materials that can be deposited onto the surfaces of medical devices [1-21].

1.4 Methods to Prevent Biofilm on Surfaces

A number of methods are currently being used to inhibit the growth of biofilm on surfaces. As reported by Singha et al. [3], numerous studies point to focusing on the prevention of biofilm rather than

on planktonic bacteria, because the slow growth of biofilms induces resistance. In their review, the investigators explore the advantages and disadvantages of popular polymeric materials used in making urinary catheters. In addition to antimicrobial capability, considerations like patient comfort, biocompatibility, mechanical strength, and sterilization must be made. The authors [3] also elaborate on the two main groups of antimicrobial agents: antifouling and biocidal. Antifouling materials are organized into two types, hydrophilic materials and polyzwitterions, both of which represent coatings that do not kill bacteria, but thermodynamically prevent the attachment of bacteria and/or proteins to the surfaces [3]. The former type repels fouling by forming a barrier of water molecules on the surface which induces a type of steric repulsion. The latter type performs physical antifouling work via electrostatic and low surface energy. Biocidal agents are designed to kill the microbes at or near the surface rather than minimize their attachment.

Existing commercially available antimicrobial catheters typically use silver alloys or antibiotic coatings. However, many other biocidal materials are currently being researched. Biocides can be categorized based on five mechanisms of action. These five biocidal mechanisms and some examples of their corresponding biocides are summarized in Table 2 [3].

Table 2: Shows five well known mechanisms to kill bacteria and the materials used to do so [3]

Category	Biocidal Mechanism	Biocide
1	Inhibition membrane synthesis	chlorhexidine, penicillin and vancomycin
2	Inhibition of protein synthesis	silver ions, nitric oxide and tetracyclines like minocycline
3	Inhibition of nucleic acid synthesis	sparfloxacin, quinolones, nitric oxide and rifampin
4	Effects on cell membrane sterols	silver ions, triclosan, antimicrobial peptides and antifungal agents like amphotericin B
5	Inhibition of unique metabolic processes	nitrofurantoin, triclosan, bacteriophages and sulfonamide

Table 2 shows that in categories 2 and 4 silver ions appear to be an effective biocide. The earliest studies using silver as a biocide for urinary catheter coatings dates back to 1949 [8]. In fact, the silver ion biocidal mechanism is comprised of multiple effects including impaired membrane function via

membrane potential, protein dysfunction by cleavage of Fe-S bonds in membrane bound protein clusters, and oxidative stress by antioxidant depletion [3]. This multifaceted mechanism of antimicrobial effects is what makes silver so potent and therefore, clinically popular. Although cutting edge research has been directed to address all mechanisms of biocidal and antifouling coatings, Sengha et al. make an important conclusion by stating that combining multi-mechanistic ingredients to form synergistic mechanisms would be the ideal approach.

Since silver is such a well-known biocide, urinary catheters coated and impregnated with silver have become commercially available and have been widely studied. In 1995, investigators [6] concluded that these devices fail to demonstrate efficacy in using silver to prevent catheter associated bacterial infection. The study used 5% silver oxide coatings tested against uncoated controls and they monitored catheter-care violations, such as disconnection of the catheter drainage tubing junction, improper positioning of the urine collection bag, and failure to clamp or sheath the outflow spigot. The onset of bacteriuria was defined as the day when the patient's urine specimen contained greater than 1000 CFU/mL of any bacteria or yeast (units CFU/mL are defined as the number of colonies of bacteria incubated in a Petri dish from a milliliter of the media in which the bacteria were initially growing). Unfortunately, the authors [6] also mentioned the occurrence of a black discharge and irritation in patients using silver coated catheters, and they advocated for more rigorous studies and safety evaluations on products that blur the line between drugs and medical devices.

In 2010, Nadkumar et al. [22] conducted a study comparing a standard latex urinary catheter, which they impregnated with silver oxide, against three brands of commercially available latex Foley catheters. This study marks the attempt to meet the demand for more rigorous studies on silver catheters. The investigators measured surface contact angles, catheter mechanical properties, silver ion release rate, cytotoxicity, and antibacterial properties. They claimed that many silver catheters are marginally effective because some companies used fine coatings that can become passivated or deactivated by proteins early on, while other companies used coatings that limited impregnated concentrations of silver from ever being exposed to the surface. The results of the study showed that numerous strains of bacteria, already

found to be resistant to antibiotics, were still sensitive to the silver. They went as far as placing submerged catheters into a centrifuge to determine the final concentration of unbound silver released into solution. The authors' results showed no toxicity to human cell lines (cytotoxicity) and only 0.0299 ppm of silver released from one gram of the catheter material, which is far below the U.S. Environmental Protection Agency toxicity guidelines (1991) set at 5 μg silver per kg of body weight per day. They also reference silver toxicity to occur at serum levels of 0.3 $\mu\text{g}/\text{mL}$ or greater, resulting in manifestation of diseases such as argyria, leucopenia, and alterations in the neural and renal tissues. Authors [7], [15] reiterate that the antimicrobial mechanism behind silver is that of soluble silver ions, which bind strongly to electron donor groups in biological molecules. E.L Lawrence and I.G. Turner [8] reported that silver concentrations of approximately 1–100 mg/L proved to be biocidal. Silver oxide impregnation was reported to result in an increase in hydrophobicity of the latex catheter surface, which is a negative property as hydrophilic materials are more resistant to bacterial adhesion than hydrophobic materials [22]. Nandkumar et al. [22] showed that urinary catheters coated with silver oxide formed large zones of bacteria inhibition on agar plates and minimal bacterial presence under fluorescent microscopy. This result points to the possibility that silver ions are able to diffuse into the agar to force a boundary of growth inhibition.

An alternative to surface coatings involves the use of electrical fields and currents [13], [15]–[19], [30]. For 2009, Del Pozo et al. [16] conducted a study with the aim to determine the effect of prolonged exposure to low-intensity, direct electrical current (DC) on *Pseudomonas aeruginosa*, *S. aureus*, and *S. epidermidis* biofilms. These infectious species are well known to be the cause of most UTIs. The investigators tested biofilm-covered PTFE coupons submerged in a slightly ionic media exposed to DC electrical current. They concluded that a higher amperage was correlated with a greater reduction of biofilm at every point in time during the study. Their results also show that electrical current can substantially reduce the viability of biofilm on a PTFE surface. They called this mechanism the electricidal effect and related the mechanism to “the disruption of the integrity of the bacterial membrane or to the generation of chlorine, oxygen, and/or hydrogen peroxide as a result of electrolysis” [16].

In 2016, Voegelé et al. [17] introduced electrical current to a catheter model via intraluminal-positioned, platinum electrodes connected to an external power supply as shown in Figure 4. Selected bacteria, cultured in an ionic media, were added to the lumen of a catheter and exposed to direct electrical current via electrodes. Statistically significant differences were detected between no electrical current exposure and electrical current exposure of 200 μA and higher for all microorganisms studied. Their results show that electrical current applied to the media with the use of intraluminal electrodes has a clear effect on biofilms aggregating on the surfaces of a PVC catheter. It has been proposed that the underlying mechanisms is due to damage to the cell walls, stress from oxygen ions and other highly oxidative compounds, changes in pH, and the formation of hypochlorous acid by electrolysis. Therefore, it can be inferred that the authors [17] suspect that the underlying mechanisms are electrochemical in nature.

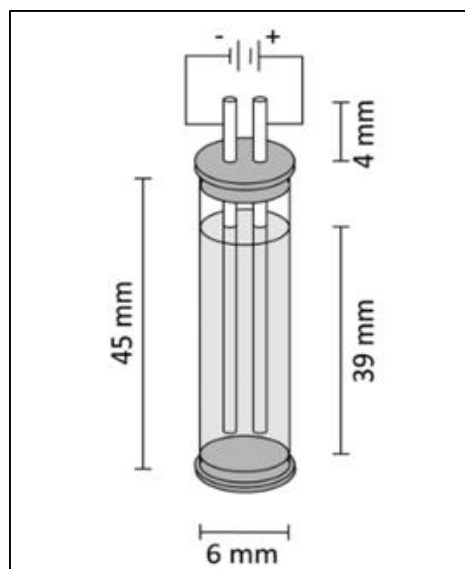


Figure 4: A diagram showing the setup for an antimicrobial electrical current experiment in a catheter model. An ionic media inoculated with bacteria is sealed in a catheter section with two endcaps and exposed to electrode potentials from a DC power source [7]

One group of inventors [12] designed an “electroceutical wound dressing” capable of generating a local field strength that is two orders of magnitude less than 100 kV/m. The term “electroceutical,” refers to a category of devices that can generate therapeutic, electric currents or fields capable of

improving impaired biological function. Caution must be observed since 100 kV/m is a strong enough field for cell membranes to become porous or to fuse with other cell membranes (electroporation and electrofusion, respectively) [30]. The disk-shaped bandage, shown in Figure 5 below, contains two electrodes that deliver current to the wound across a hydrogel interface, from a DC coin cell power source. It is important to make the distinction between wound-healing and antimicrobial electroceuticals. Wahlsten et al. [30] compared simulations of bandages that produce microcurrents *with respect to the surface charge of wounded skin*. They omitted the connection to microcurrents as an antimicrobial and instead focused on wound healing capabilities.



Figure 5: A photo of an electroceutical, wound therapy bandage. A flap is pulled back to reveal the central cathode on the wound viewing window which is connected in series to the outer anode [31]

The results from studies presented by Voegelé [17], Del Pozo [16] and Singha [3] all suggest bacteria are responsive to electrochemical changes. This suggests that any electrochemical or galvanic action can be used to inhibit biofilm formation by creating changes in pH and concentrations of ions on surfaces. A separate, but unique study discusses efforts to control the *in vitro* corrosion of a biodegradable magnesium alloy for orthopedic applications. Magnesium alloys would readily dissolve into soluble ions in an ionic aqueous solution, which has inspired biomaterial researchers to develop them into a new kind

of bio-absorbable material [32]. The mineral ions found naturally in the tissues and vessels were capable of generating continuous electrochemical reactions at the surface of the alloy. For a list of minerals used by cells in the human body, please refer to Table 4 [33]. In the case of a Mg-Ca alloy, Li et al. [32] explained that the alloy dissociates into products that become available to both signal cells and physically build bone. One experiment showed gradual degradation of a Mg-Ca osteoimplant *in vivo* within 90 days, leaving newly formed bone. Gu et al. reported that the calcium used in this alloy can even be substituted with zinc or a list of other metals [34]. A similar electrochemical reaction was achieved by authors [35] who combined palladium and silver. A silver coupon plated with a screen-like coating of palladium is said to create a galvanic cell in an ionic solution, releasing silver ions into the solution. The authors show a strain of silver-sensitive bacteria growing colonies on a pure silver surface and not on the silver-palladium surface. Although not all metals have the same reactivity in solution, these examples offer the notion that dissimilar metals can be used *in situ* to generate passive reduction/oxidation reactions, or redox reactions.

Choosing the right metals to form a reaction in the human body requires careful consideration. Table 3 may be helpful in selecting potential active materials as it contains a list of minerals that are used biologically. For example, magnesium and calcium are essential macrominerals, but require careful alloying and are dangerously reactive in pure forms and in larger quantities. Palladium and silver are not essential for biological function and can be costly and toxic, respectively. However, zinc is an essential mineral for humans and is a widely used active ingredient in topical antimicrobial solutions [26], [33]. This essential nutrient is used by cells in many central processes including apoptosis regulation [36]. Thermodynamically speaking, zinc has very strong potential to reduce other materials (to become oxidized) [37].

Table 3: A table showing minerals used in the human body. Some minerals are more essential than others and some are used in trace by coexisting microorganisms[33]

Mineral Type	Evidence	Mineral
Macrominerals		
Essential Abundant Elements	Required in gram quantities per day	Calcium Magnesium Phosphorus Potassium Sodium Chlorine
Trace Minerals		
Essential Trace Elements	Required in milligrams quantities per day	Boron Copper Magnesium Manganese Zinc
Essential Ultra Trace Elements	Required in microgram quantities per day	Chromium Cobalt Iodine Molybdenum Selenium
Possibly Essential Ultra Trace Elements	Apply to the following four main groups of circumstantial evidence: 1)A dietary deprivation in some animal model consistently results in a changed biological function, body structure, or tissue composition that is preventable or reversible by an intake of an apparent physiological amount of the element in question. 2)The element fills the need at physiological concentrations for a known in vivo biochemical action to proceed in vitro. 3)The element is a component of known biologically important molecules in some life forms 4)The element has an essential function in lower forms of life.	Arsenic Nickel Silicon Vanadium Aluminum
Other Elements with Beneficial or Biological Actions	Apply to one or two of the main groups of circumstantial evidence	Bromine Cadmium Fluorine Germanium Lead Lithium Rubidium Tin

An investigation by Sawai et al. [38] in 1998 showed that some metallic oxide powders have been found to inhibit bacterial growth, one example being zinc oxide. They have shown in previous work that zinc oxide acted on gram-positive bacteria more strongly than on gram-negative bacteria. More importantly, they observed the generation of hydrogen peroxide from zinc oxide powder slurry. They find that the use of zinc oxide in conjunction with antibiotics showed improved antibiotic performance, which is attributed to membrane permeable hydrogen peroxide generated by the zinc oxide in solution [38]. In an aqueous solution, zinc metal can be oxidized by dissolved oxygen, the result of which may go on to produce hydrogen peroxide. These examples point to the possibility of using electrochemically active materials in the body that could potentially react with ions in the tissue and generate an active surface too hostile for bacteria. A study conducted by Banerjee et al. [18], [19] shows the ability of an antimicrobial wound dressing to do just that.

The aforementioned antimicrobial wound dressing is a commercial product also characterized as an electroceutical, but one that inhibits infection. Banerjee et al.[18] used numerous experiments to characterize the wireless or bio electric dressing. The bio electric dressing seen in Figure 6 is composed of a polyester wound dressing imprinted with a regular pattern of circular zinc and silver electrodes. The zinc anodes are 1mm in diameter, the silver cathodes are 2mm in diameter, and the electrodes have a 1mm separation.

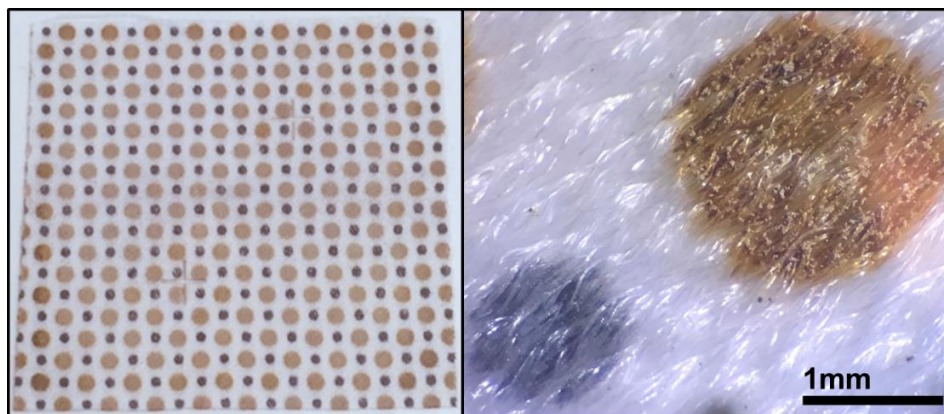


Figure 6: Photos of Zn/Ag bioelectric wound dressing (top) composed of zinc electrodes 1mm OD (grey) and silver electrodes 2mm OD with a 5mm lattice parameter (bottom).

A bio electric dressing imbedded into agar plates dramatically reduced bacterial growth ($n=4$, $p<0.001$). The bio electric dressing significantly attenuated cell aggregation and demonstrated absence of biofilm-like structures and thinner biofilms. Their results show that, overall, the bio electric dressing caused bacterial cell death and decreased extracellular polymeric substance [18]. The underlying biocidal properties were multi-mechanistic based on a wide number of experiments performed on the bio electric dressing. First, Banerjee et al. [18] attributed some of the biocidal effects to silver. However, they also suggest that the concentration of silver required to eradicate the bacterial biofilm in chronic wounds would be cytotoxic. Using electron paramagnetic resonance, they measured the spontaneous micromolar superoxide production by the bio electric dressing in phosphate buffered saline at room temperature. It is possible that in an ionic aqueous environment saturated with oxygen, superoxides would be expected to rapidly form hydrogen peroxide. The specific reaction occurring between the zinc and the silver forms a synergy that somehow improved its biocidal properties. Finally, in a separate experiment they [18] found that the bio electric dressing inhibits glycerol-3phosphate dehydrogenase activity, which is a protein that protects the cell reactive oxygen species. This result suggests that electric fields may have an effect on molecular charge distributions on cellular machinery often found in membranes.

The bioelectric reaction described earlier, shows signs of synergy between two active ingredients which perpetuate a multitude of possible antimicrobial mechanisms. In a separate study, Banerjee et al. [19] described the nature of a zinc-silver bioelectric wound dressing and its ability to signal cells for wound healing and disrupt biofilm formation. They explained that the main electricidal mechanism is from “ambipolar diffusion” occurring as a result of the electric field associated with adjacent, oppositely charged electrodes in contact with a conductive medium. This diffusion is defined by a collection of electrons and ions with differing masses and charge that move with a diffusivity lesser than that of electrons but greater than that of positive ions [19]. The authors hypothesized that when the bio electric dressing is in contact with an aqueous solution, the silver is the cathode and becomes reduced, and the zinc electrode is the negative cathode and becomes oxidized. But electrochemically speaking, this is highly unlikely. In fact, silver cannot be reduced in an ionic solution without a bias current; silver oxide,

however, can be. For this reason, Banerjee and the other investigators added to the theory by postulating that a set of redox reactions are expected to occur in an aqueous media. In the reactions, silver (I and II) oxides react with water, which is important because the reaction should not be confused with solubility of silver, but with electrochemical reactions occurring at the oxidized surface. Indeed, no applied electric field is required to drive these reactions.

Additionally, Banerjee et al. shows that the zinc-silver bio electric dressing generates hydrogen peroxide in PBS and the amount produced increases with increasing size of the dressing [19]. This observation may confirm the reason behind why the bio electric dressing is able to inhibit bacterial growth even when the authors submerged the dressing under 2 mm of agar. This suggests that some agent is able to diffuse through the agar as the proposed electric fields would be too weak to affect bacteria above a layer of agar. Hydrogen peroxide has been shown to inhibit bacteria such as *E. coli* and *S. faecalis* at certain concentrations [39]. The inhibition of bacteria caused by the products of a redox reaction combined together with the electric fields and ions that signal cells to migrate, makes the zinc silver model perfect for wound care. This mechanism is similar to how the corrosion of a Mg-Ca alloy implant results in bioavailability of magnesium and calcium ions, which recruit cells and provide the minerals necessary for bone formation [32]. However, since oxidative stress occurs often in aerobic conditions, organisms have evolved to have large concentrations of very efficient enzymes that manage hydrogen peroxide, the peroxide anion, and superoxides, rendering them less susceptible to oxidative treatments [14][40].

The zinc-silver reactions used in the bio electric dressing have the ability to propagate a biofilm inhibiting effect and may be an ideal solution when applied to a urinary catheter because the passive electricidal nature of the model requires no wiring or external power supply. For this purpose, the aim of this thesis is to design a urinary catheter coating with combinations of the active materials containing zinc and silver for biocidal purposes.

Chapter 2: Selection of Active Materials and Rationale

As noted in the preceding chapter, the zinc-silver redox couple has been shown to possess many effects that inhibit bacterial growth. Although the exact mechanism inhibiting the bacterial growth is still unknown, the zinc-silver redox couple provides a unique model for a passive, electricidal coating. This model is advantageous because the effects can be produced electrochemically without requiring additional wiring or an external power source. An electrochemical reaction is defined as “any process either accompanied by the passage of an electrical current and involving in most cases the transfer of electrons across an interface of two [usually heterogeneous] substances”[41]. Some relevant half-reactions involving silver and zinc in an aqueous solution have been selected from the electrochemical series [42] and are listed along with their standard reduction potentials in Table 4. Urine is an aqueous substance that contains many additional species such as dissolved oxygen (O_2), sulfate anion (SO_4^{2-}), chloride anion (Cl^-), and other biological compounds. Some half-reactions containing dissolved oxygen, chloride anions, and sulfate anions have also been listed to show other possible half-reactions that may also involve silver and zinc. The reduction potentials in this table are relative to the standard hydrogen electrode (SHE), with reactants and products at room temperature and unit activity.

Table 4: List of half-reactions selected from the electrochemical series relevant to using the zinc-silver redox couple as a surface coating in an aqueous solution [42]. The standard reduction potentials are relative to the standard hydrogen electrode, at room temperature and unit activity.

Half-Reaction	Reduction Potential, E° (V)	#
$\text{Ag}^+ + \text{e}^- \leftrightarrow \text{Ag}$	+0.7996	(1)
$\text{Ag}_2\text{O} + \text{H}_2\text{O} + 2\text{e}^- \leftrightarrow 2\text{Ag} + 2\text{OH}^-$	+0.342	(2)
$2\text{AgO} + \text{H}_2\text{O} + 2\text{e}^- \leftrightarrow \text{Ag}_2\text{O} + 2\text{OH}^-$	+0.739	(3)
$\text{Zn}^{2+} + 2\text{e}^- \leftrightarrow \text{Zn}$	-0.7618	(4)
$\text{ZnO} + \text{H}_2\text{O} + 2\text{e}^- \leftrightarrow \text{Zn} + 2\text{OH}^-$	-1.260	(5)
$\text{Zn}(\text{OH})_2 + 2\text{e}^- \leftrightarrow \text{Zn} + 2\text{OH}^-$	-1.249	(6)
$\text{O}_2 + \text{H}_2\text{O} + 2\text{e}^- \leftrightarrow \text{HO}_2^- + \text{OH}^-$	-0.076	(7)
$\text{O}_2 + 2\text{H}_2\text{O} + 2\text{e}^- \leftrightarrow \text{H}_2\text{O}_2 + 2\text{OH}^-$	-0.146	(8)
$\text{AgCl} + \text{e}^- \leftrightarrow \text{Ag} + \text{Cl}^-$	+0.22233	(9)
$\text{Ag}_2\text{SO}_4 + 2\text{e}^- \leftrightarrow 2\text{Ag} + \text{SO}_4^{2-}$	+0.654	(10)

For practical purposes, activity of gaseous reactants is approximated by their partial pressure, and activity of solutes is approximated by their molar concentrations. If the reactants exist as a pure solid or liquid, their activities are defined as unity (activity = 1). Positive potentials in Table 4 signify that the reduction half-reactions are thermodynamically favored to proceed from left to right, whereas negative potentials indicate that the half-reactions are thermodynamically favored to proceed from right to left. If the reactant concentrations deviate from unit activity the reduction potential will change. For example, the reduction potential of a generalized half-reaction [43] such as



where e^- represents the electron, A, B, C, D identify the chemical formula of the reactants, and coefficients $a, b, c, d,$ and n represent the respective molar quantities of the reactants, products, and electrons participating in the reaction, will be given by the Nernst equation [43]:

$$E = E^0 - \frac{RT}{nF} \ln \frac{[C]^c[D]^d \dots}{[A]^a[B]^b \dots} \quad (12)$$

In Equation 12, E^0 is the standard reduction potential of the half-reaction, T is temperature, F is the Faraday constant, and $[A],[B], [C]$, and $[D]$ represent the molar concentrations of the respective reactant and products; as indicated above, concentrations are used to approximate the activities. It is important to note that half-reactions do not occur independently but require coupling to another half-reaction to achieve electrical charge balance. The net reaction is determined by combining appropriate half-reactions and the thermodynamic tendency for the net reaction to proceed in a given direction is determined by the polarity and magnitude of the sum of half-reaction potentials; this will be demonstrated in subsequent paragraphs.

The Nernst equation has been used to produce Pourbaix diagrams [37], which conveniently define the stable forms of various metals and their reaction products in aqueous solutions at various potentials with respect to pH. Pourbaix diagrams for zinc and silver are shown in Figures 7 and 8, respectively. In these diagrams the thermodynamically stable region of water lies between dashed lines labeled ‘a’ and ‘b’. In the region below the ‘a’ line, hydrogen gas is liberated from solution and above the ‘b’ line oxygen is liberated. The solid lines plotted in each diagram define boundaries between the various preferred states of the metals. As implied by the Equation 12, these boundaries are a function the reactant concentrations. The un-circled numbers associated with each solid line represent the \log_{10} values of the reactant activities. It must be understood that the pH and electrode potentials are those present at the metal-solution interface, and not in the bulk solution. Pourbaix diagrams assume the absence of competing reactions not reflected in the diagrams and deposition onto interfaces which would interfere with equilibria at the interfaces.

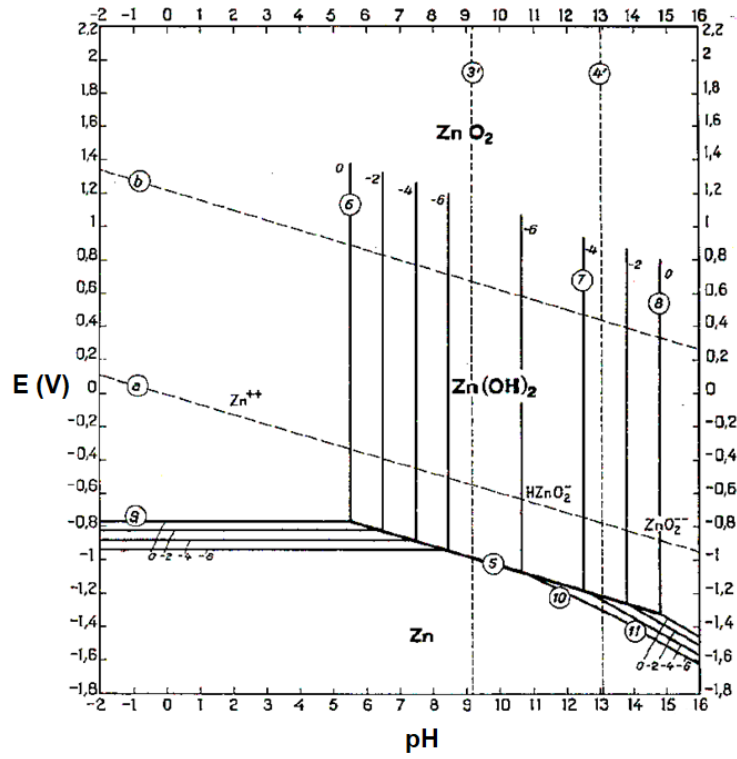


Figure 7: Pourbaix diagram for zinc in aqueous solution [37]

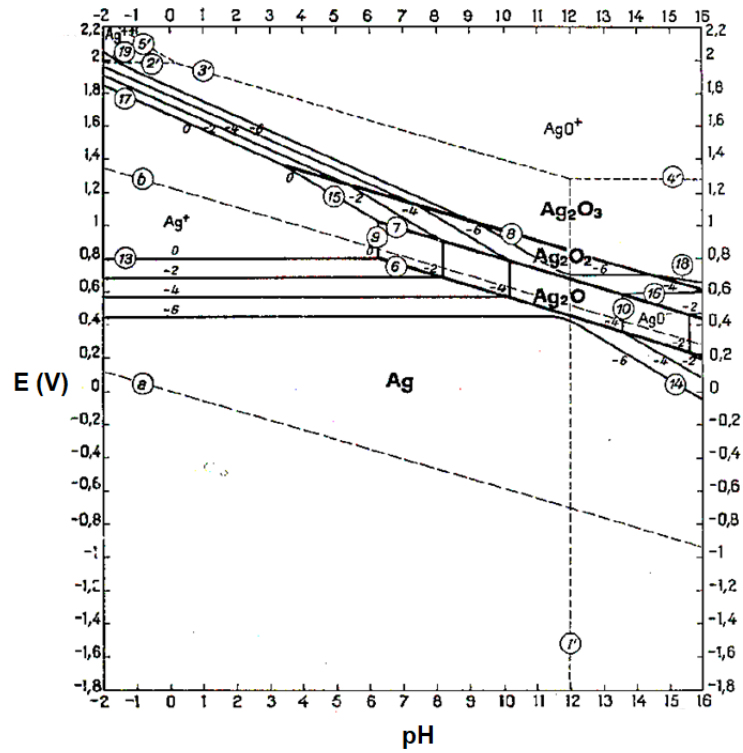


Figure 8: The Pourbaix diagram for silver in aqueous solution [37]

One can therefore use half-reactions 1-6 in Table 4 to demonstrate the thermodynamic favorability of zinc metal to reduce both silver (I) oxide (Ag_2O) and silver (II) oxide (AgO) to silver metal. For the case of Ag_2O reduction, this is shown by combining reactions 2 and 5 as follows:



Because reaction 5 was inverted, the polarity of its potential has also been inverted, given as reaction 5'. The resultant potential for the overall reaction (assuming unit activity), ΔE_{cell} , is positive, demonstrating the tendency to proceed from left to right. The magnitude of the potential would change according the Nernst equation if the molar concentrations of OH^- deviated from unity. Equation 13 is also the driving equation for a silver-oxide battery.

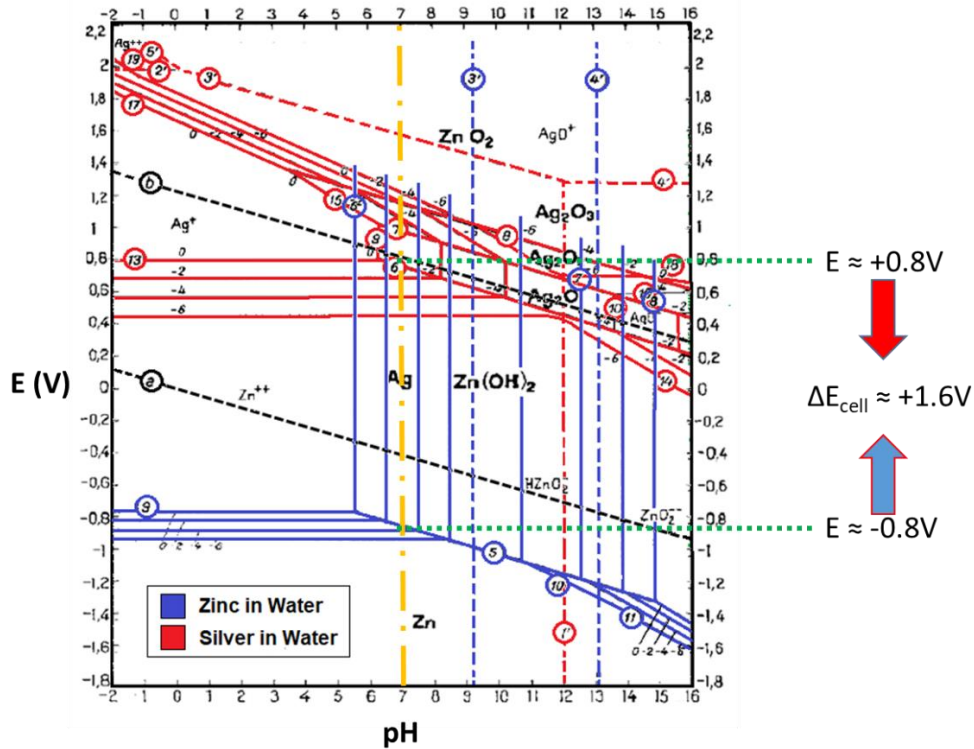
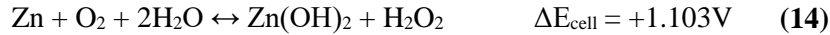


Figure 9: Superimposed Pourbaix diagrams of zinc (blue) and silver (red). At a pH of seven the potential of the overall reaction is +1.6 volts

From inspection of superimposed silver and zinc Pourbaix diagrams, as shown in Figure 9, one can immediately see that in the absence of a direct electrical connection a potential difference of approximately positive 1.6 volts exists between a silver surface coated with Ag₂O and a zinc metal surface immersed in water at pH ≈ 7 (urine) in agreement with Equation 13. This represents an open circuit condition where no electrical current is allowed to flow. In the open circuit condition, an electric field is created between the metal surfaces similar to what authors have described in the zinc-silver bio electric dressing. If, however, the Ag₂O coated surface is electrically connected to zinc metal, the Ag/Ag₂O surface will act as a cathode and zinc will act as anode. Under these conditions, the reduction process will proceed as long as Ag₂O is present. Once Ag₂O is completely consumed and only silver metal is present at the metal-solution interface, the overall reaction defined in Equation 13 terminates; at this point other reactions may occur. One possible thermodynamically favored process on the surface of zinc in the presence of dissolved oxygen, is the reduction of dissolved oxygen to form hydrogen peroxide as shown below.



The new standard cell potential, $\Delta E_{\text{cell}} = +1.103\text{V}$ may allow for spontaneous reduction of oxygen into hydrogen peroxide in the presence of zinc or zinc hydroxide if the solution is saturated with oxygen. Figure 10 displays a simplified Pourbaix diagram showing the regions of stability of water. At a pH of roughly seven, any metal surfaces with equilibrium potentials below 0.6 volts can participate in the reduction of soluble oxygen into hydrogen peroxide. Hydrogen peroxide and peroxide anions are reactive oxygen species that are harmful to many organisms at certain concentrations [14], [39].

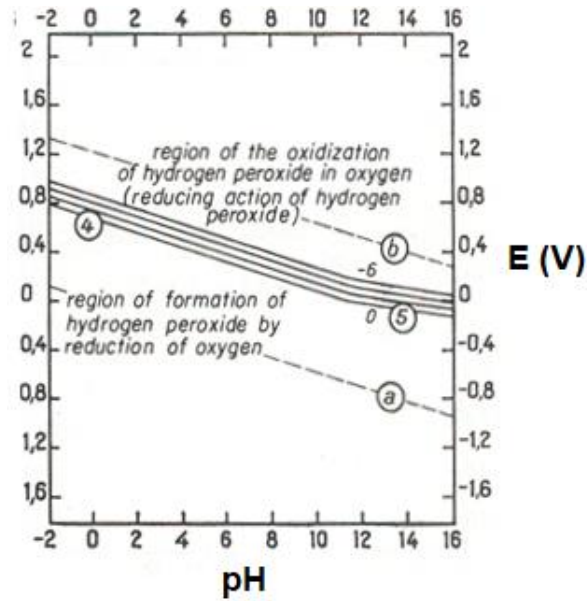


Figure 10: A Pourbaix diagram showing the regions of stability of water [37]

In electrochemistry, reactions involve overcoming activation barriers where energy is transferred from one state to another, governed by thermodynamics. However, the fact that a reaction is thermodynamically possible, does not mean it will take place. This would occur only under the assumption that these reactions are reversible, but electrochemical reactions are highly conditional and may occur irreversibly. As noted above, Pourbaix diagrams are based on thermodynamics and assume the absence of competing reactions not reflected in the diagrams. The intended reactions of the zinc-silver model are limited by competing reactions as well as other kinetic processes. The reaction rates and current at the electrode surface can be described by kinetics in a series of steps (Figure 11). For an electrode reaction $O + ne^- \leftrightarrow R$, these steps cause the conversion of the dissolved oxidized species, O to reduce to form, R, also in solution. The electrode reaction rate is governed by a combination of rates from the following processes [44].

1. Mass transfer of chemical species to and from the bulk solution
2. Electron transfer at the electrode surface

3. Heterogeneous/homogeneous chemical reactions on the electrode surface occurring before/after the electron transfer
4. Surface reactions corresponding to adsorption, desorption, and/or crystallization/electrodeposition

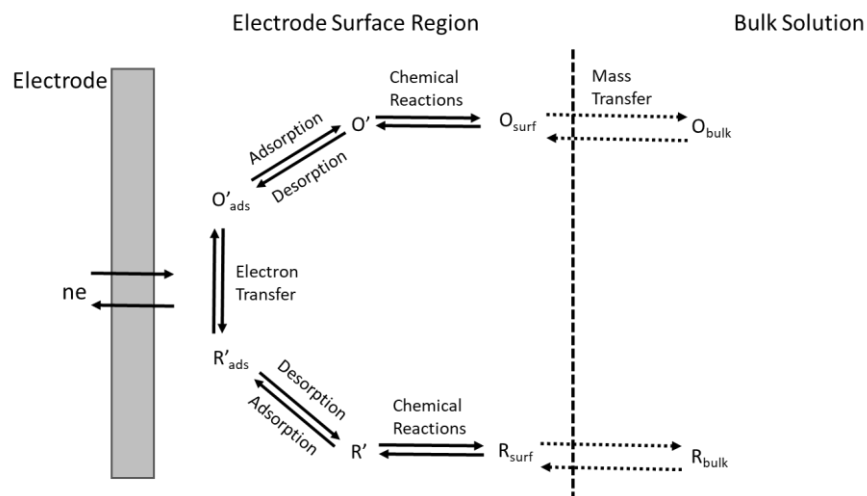


Figure 10: A series of kinetic steps limiting the overall electrode reaction rate

These time dependent steps may limit the rate of the electrochemical reaction. Overall, the migration of these species between electrodes can be impeded by attachment losses, recombination, and chemical reaction; this makes the determination of current flow dynamics very complicated. Since the electrodes are envisioned to be physically scattered about the surface of a urinary catheter, solving the reaction kinetics at the surface is beyond the scope of this thesis. Additionally, it is important to note that bodily fluids, especially urine, must act as the electrolyte for the catheter to function. In addition to H^+ and OH^- ions there are other electrolytes (e.g. Na^+ , Ca^{2+} , Cl^- , Mg^{2+} , K^{2+}) and other biological compounds (e.g. proteins, uric acid, lactic acid, citric acid, sodium bicarbonate, ammonium chloride). Equations 9 and 10 in Table 4 give two examples of other possible half-reactions involving zinc and silver relevant to urine. It is possible that of these species and others are capable of reacting with and creating a passivation layer that inactivates the surface of the zinc and silver oxide electrodes. On the other hand, these ions can

also react with electrode surfaces to produce other chemical species. The real challenge of this project is effectively combining the active materials with commercial urinary catheter materials, to produce a new material with surfaces capable of perpetuating the electrochemical reactions for an extended time, following exposure to bodily fluids. Urologists have suggested that it would be a major accomplishment to design a catheter with surfaces that maintain sterility for 30 days, since 100% of patients would develop a bacterial infection by that time [8][26].

An additional, important design constraint for urinary catheter surfaces is wettability or the ability of a liquid to make contact with a solid surface due to the intermolecular forces between them. Depending on how much active materials are available at the surface, changes in surface wettability (hydrophobicity/hydrophilicity) are also expected. The wettability of the catheter influences both growth of biofilm on the surface and the comfort of a patient using the catheter. Studies have suggested that interactions between bacterial cell walls and other surfaces are affected by electrostatic interactions and Van der Waals forces [28]. Studies regarding the adhesion of different strains of *E. coli* have also found that they are highly attracted to hydrophobic surfaces, while being slightly repelled by hydrophilic ones [45]. Furthermore, catheters coated with hydrophilic materials also reduce trauma to the urethral surfaces and enable easy and comfortable catheterization for patients, as compared to more hydrophobic conventional catheters [25]. As such, measuring the wettability of the catheter coatings is both important for the prevention of biofilm formation and improvement of patient comfort. One of the most optimal methods to measure the wettability of a surface measuring the contact angle that a droplet of liquid forms with that surface, as shown in Figure 11. A contact angle between zero and 90 degrees (Figure 11A/B) would indicate high wettability and a hydrophilic surface, whereas a contact angle between ninety and 180 (Figure 11C/D) indicates low wettability and a hydrophobic surface [46].

To conclude, all considerations suggest that the more stable species, silver (I) oxide, is needed for the reaction to proceed if electrochemical in nature. The unique interaction of zinc and silver (I) oxide in solution creates an interfacial environment that is potentially too chaotic for bacteria to manage. At the surface of the urinary catheter, bacteria may be interacting with changes in pH, electric fields, micro-

currents generated from the ions caught in electric fields, toxic metal ions, and reactive oxygen species. The zinc-silver couple is, therefore, an obvious candidate for an antifouling/biocidal surface treatment.

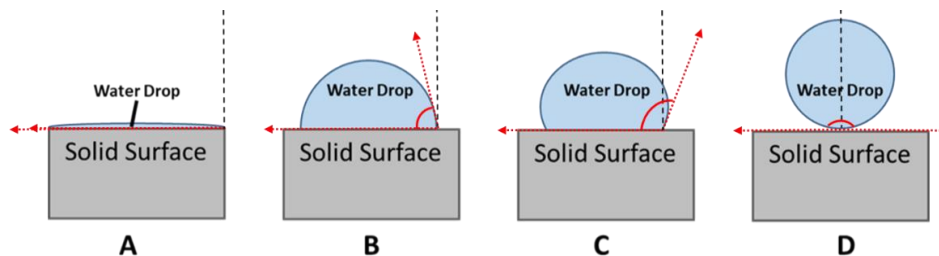


Image	Contact Angle (°)	Degree of Wetting	Solid-Liquid Interaction Strength
A	0	Perfect Wetting	Strong
B	$0 < \theta < 90$	High Wettability	Middle
C	$90 < \theta < 180$	Low Wettability	Weak
D	180	No Wetting	Weak

Figure 11: An illustration of the degree of surface wettability based on the contact angle formed between a liquid drop and the solid surface

Chapter 3: Catheter Coating Formulation and Coating Methods

3.1 Materials Used for Fabricating Urinary Catheters

A wide variety of materials is used to manufacture medical devices, each with their own defined manufacturability, physical properties, and use regulations. Catheters are made exclusively from polymers due to the physical and chemical properties characteristic of polymers [3], [8], [47]. Certain polymers can be produced to be light weight, non-reactive, elastic, and easily formed. A list of polymers widely used for making medical devices can be seen in Table 5 [47]. These polymers can take on varying formulations and have a number of additives depending on the application. Additives include but are not limited to: fillers, reinforcements, release agents, internal lubricants, catalysts, impact and toughness modifiers, thermal and radiation stabilizers, plasticizers, pigments, coupling agents, and antistats. All additives play a role in manufacturing the device, as well as how the final device will behave.

Table 5: A table of polymers used to make medical devices. Polymers PVC, Silicone, TPU, PEEK, have been used to make catheters [47]

Polymer	Abbreviation	Useful Properties and/or Applications
Polyethylene	PE	Wide variety, with adjustable properties
Ultra-low-density	ULDPE	densities ranging from 0.890 to 0.905 g/cm ³ contains comonomer.
Very-low-density	VLDPE	densities ranging from 0.905 to 0.915 g/cm ³ contains comonomer
Linear-low-density	LLDPE	densities ranging from 0.915 to 0.935 g/cm ³ contains comonomer
Low-density	LDPE	densities ranging from about 0.915 to 0.935 g/cm ³
Medium-density	MDPE	densities ranging from 0.926 to 0.940 g/cm ³ may or may not contain comonomer
High-density	HDPE	densities ranging from 0.940 to 0.970 g/cm ³ may or may not contain comonomer.
Ultra-high-molecular-weight	UHMWPE	>0.970 g/cm ³ Used for hip and knee implants for wear resistance
Polypropylene	PP	Wide variety, with adjustable properties
Homopolymer		Stiffest of the three types; used in thermoforming, slit film and oriented fibers, drapes, gowns, sutures
Random Copolymer		The most flexible and clear of the three types; household items, containers for food and chemicals
Impact Copolymers		Block polymer made to increase impact strength; film, sheet, high-press. resistance, thin-wall parts
Polystyrene	PS	Disposable laboratory ware, diagnostic instruments
High Impact	HIPS	Laboratory ware and medical devices
Syndiotactic	SPS	Films for improved gloss, aesthetics
Polyester and Liquid Crystal Polymers	PE	Wide variety, with adjustable properties
Polycarbonate	PC	Clear as glass, resistant to impact, UV, and heat; Serializable medical apparatus
Poly(ethylene terephthalate)	PET	Most common type: bottles, packaging, clothing
Poly(butylene terephthalate)	PBT	Packaging, syringe pump components, dental instruments
Poly(lactic acid)	PLA	Biodegradable devices: sutures, implants, drug-delivery devices, tissue engineering
Poly(glycolic acid)	PGA	Quick dissolving polymer, can be blended with PLA to control dissolution

Table 5 Cont. : A table of polymers used to make medical devices. Polymers PVC, Silicone, TPU, PEEK, have been used to make catheters [47]

Polymer	Abbreviation	Useful Properties and/or Applications
Poly(vinyl chloride)	PVC	Most widely used plastic resin in medical devices, due to low cost ease of processing, and ease of tailoring its properties for range of applications
Poly(ether sulfone)	PES	High temp performance ($T_g=224C$), low mold shrinkage; medical equipment requiring repeated sterilization
Polysulfone	PSU	Similar to PES, also high toughness and strength, fire resistant, transparent; membranes and fluid handling applications
Poly(methyl methacrylate)	PMMA	Optically clear and colorless, extremely hard surface, impact and abrasion resistant; valves, housings, PPE, catheter accessories
Poly(ether etherketone)	PEEK	Young's modulus of elasticity is 3.6 GPa and tensile strength is 170 MPa; Outstanding resistance to chemicals, wear, hydrolysis, radiation mechanical properties, thermal properties; Very good dielectric strength, volume resistivity, tracking resistance; used for implants, and reusable medical components
Poly(p-xylylene)	Various	Polymerized onto surfaces using vapor phase deposition of monomers; coatings for implants, needles, and prosthetic devices
Polytetraflouroethylene	PTFE	Resistant to temperature ($T_m = 320C$), very smooth; Catheter coatings, fittings, valves, tubing, dielectrics
Polyorganosiloxane (Silicone)	Various	Elastic, resistant to temperature moisture and chemicals; Prosthesis, artificial organs, contact lens, microfluidics
Thermoplastic Elastomers	TPE	Physical and chemical properties can vary depending on how the monomers are varied; Amorphous, low Young's modulus and high yield strain; applications vary
Polyamide TPE	TPA	
Copolyester TPE	TPC	
Olefinic TPE	TPO	
Urethane TPE	TPU	
Styrenic TPE	TPS	
Thermoplastic rubber vulcanizate	TPV	
Unclassified TPE	TPZ	

Catheters are devices that direct flow of bodily fluids from into, out of, or through, various passages of the body. A urinary catheter is intended to be deployed into the urinary tract of a patient with urinary incontinence. A Foley's urinary catheter (Figure 1) has two separate lumens and ports: one set to flush urine from the bladder, and one set to inflate the balloon at the distal end of the catheter. The balloon is designed to inflate in the bladder and prevent the catheter from inadvertently slipping out from the patient. In a review on the materials for urinary catheters, E.L Lawrence and I.G Turner [8] explain that, aside from biocompatibility, the most important constraints are a smooth surface finish and proper flexibility. In other words, mechanical trauma and shear forces at the biomaterial-tissue interface are to be kept to a minimum. To add, the catheter must be stiff enough not to compress or kink by the body's weight, yet flexible enough as not to perforate tissue. Vulcanized natural rubber latex has become increasingly unpopular due allergic reactions with human tissue [26]. The silicone elastomer polydimethyl siloxane (PDMS) is inert, biocompatible, and flexible alternative [3]. The mechanical properties can be varied depending on how much cross-linker is used for the polymerization reaction [48]. For this reason, PDMS was selected as the ideal substrate to combine with our active materials. Methods to formulate a coating from the active materials and PDMS so that they behave similarly flexible silver oxide batteries are described, hereafter

3.2 Methods to Incorporate Active Materials into a Catheter Coating

Methods to combine the active ingredients with the polymer in a way that they react with bodily fluids similarly to galvanic reactions in flexible silver oxide batteries [49]–[54] were investigated first. However, these methods involved toxic reagents, and were performed specifically to improve electrical power storage in batteries. Methods that can be used to form a composite of the active materials with PDMS, specifically, include chemical adhesion, chemical-free adhesion, and *in situ* synthesis. These categories exist as a result of the nature of adhesion between a metal and PDMS. Covalent bonding of silicone elastomers on metallic substrates is difficult due to an incompatible surface chemistry. Adhesion can be promoted by the use of chemical coupling agents (primers) such as: organotitanates, amide/imides,

zircoaluminates, organosilanes, etc. [55]. The mechanism of adhesion using a metal primer is illustrated in Figure 12. The primer has binding affinity for both the metal and the silicone.

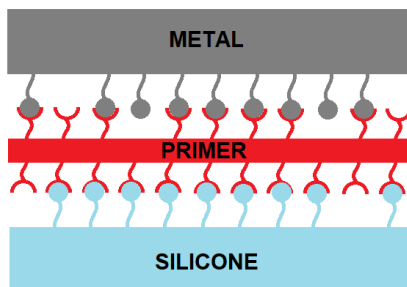


Figure 12: A depiction of how a primer is used to bond materials that have trouble physically bonding

This method requires advanced chemistry experience and the use of toxic reagents. Nandkumar et al. were able to use a chemical solvent and dissolved silver to impregnate latex Foley catheters [22]. This method uses only silver as an active ingredient. It uses a different substrate (Latex), and still involves the use of strong reagents. Thus, chemical-free adhesion and *in situ* synthesis method is a more attractive method for making the zinc-silver, PDMS composites. Goyal et al. [56] prepared a homogenous mixture of silver metal salt, silicone elastomer and the curing agent to produce metal nanoparticle embedded PDMS films. During the curing process, the hardener simultaneously crosslinks the elastomer and reduces the metal salt to form silver nanoparticles *in situ*. Although the authors' results show a reduced bacteria concentration in solution following exposure to the material, it is assumed that silver ions that have not agglomerated together are able to escape the surface of the polymer matrix. In other words, the bacteria are most likely being affected by residual silver ions, not by nanoparticle interaction.

It is a common practice to fully embed fibers in a resin when making a composite. A suspension of particles, flakes or fibers in a thermoset polymer is considered to be a composite, especially when the mechanical properties are improved [47]. In the case of the composite presented herein, it is necessary to have the active material in contact with the surface of the polymer matrix, rather than fully encompassed by it. This leads to the next method of adhesion, mechanical. In this method, a powder or metal thin film

is partially incased in PDMS and thermally bonded. This adhesion is analogous to a boulder being partially buried in the earth; the particle is buried by the polymer enough to keep it static, but still exposed. As illustrated in Figure 13, Domin Koh et al. [57] used a lithography-based method where a thin film of metal was evaporated onto chromium coated glass, etched into an electrode, and then coated in PDMS; the cured PDMS was able to be freed from the chromium with the metal electrode imbedded at the surface. The method illustrated in Figure 13 is tempting because it would allow a detailed, highly controlled pattern of silver and zinc to be deposited onto a surface and partially combined with the surface of PDMS. However, the process is still costly, and requires zinc ingots to be evaporated into a thin film; this metal was forbidden from being evaporated in the campus cleanrooms to prevent contamination.

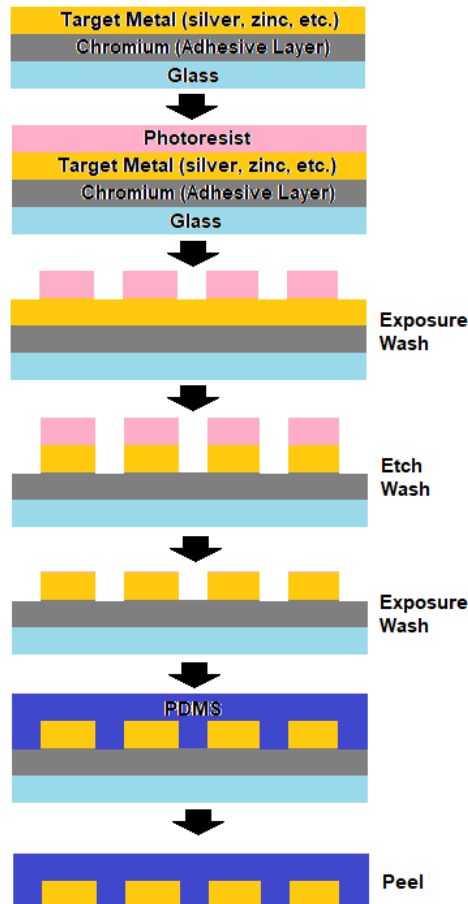


Figure 13: A schematic showing one method to imbed metal electrodes in the surface of PDMS. A combination of soft and photo lithography

The method used to make the final prototype biomaterial combines the last two methods described. PDMS monomer, cross-linker and a powdered form the active materials are combined, and thermally cured. It is important to take into consideration the previous notion that active materials will not react with the solution at the surface if they are completely encased in the polymer matrix. For this purpose, the idea of a percolation threshold is employed. At some ratio, the mass of the powdered metals will be high enough to conduct through the PDMS [58]–[60]. If this conduction can be measured at the surface than it is very likely that the active materials are available at the surface. This method can be done with zinc and silver, but since silver oxide is not good conductor, finding the proper ratio was found iteratively through AMR testing.

3.3 Preparation of Coatings and Thin Film Samples

The active ingredients zinc, silver, and silver (I) oxide are first prepared into pastes using PDMS, and then cured into films or coatings. These methods are performed as follows:

1. PDMS monomer is mixed with 14.3 %wt. cross-linker and vacuum degassed [48].
2. Silver powder (-100 mesh 99.99%) is mixed with silver (I) oxide powder (99.99%) at [2:1] molar in a separate container.
3. Individual active materials and PDMS are weighed and mixed on clean glass panes (Figure 17A).
4. Combinations of active materials were weighed and mixed on the same glass pane using the following AM:PDMS mass ratio (Figure 17B)
 - Zinc:PDMS – 4g:1g
 - Silver:PDMS – 3g:1g
 - Silver (I) oxide:PDMS – 1g:1g
 - Silver / silver (I) oxide:PDMS – 3g:2g
5. Zinc / Silver (I) Oxide:PDMS were prepared by
 - First, mixing together 0.400g of zinc with 0.200g PDMS
 - Then, mixing 0.141g of silver (I) oxide into Zn:PDMS

6. A PETG mask, 0.010” inches thick, is adhered to the glass with drops of 100% ethanol and a strip of Kapton tape.
7. The AM:PDMS pastes are poured into the well(s) formed by the mask (Figure 14C)
8. The paste is spread across the well (Figure 14D)
9. Mask is removed carefully (Figure 14E)
10. Glass panes are placed in 125 Celsius degree oven for 15 min
11. Samples are diced into 10mm x 12mm rectangles, or 8mm discs (Figure 14F)

Table 6 shows a matrix of the active materials, with check boxes to denote which were fabricated. Figure 14 shows images of process used to make a Zn:PDMS film. Figure 15 shows composite films (left to right, top to bottom) Zn, Ag, Ag₂O, Ag-coated catheter, Ag/Ag₂O, Zn/Ag₂O mixed, Zn/Ag₂O patterned, and a bio electric dressing.

Table 6: Check boxes represent the following combinations of active materials that were studied

	Zn	Ag	Ag ₂ O
Zn	✓		✓
Ag		✓	✓
Ag ₂ O	✓	✓	✓

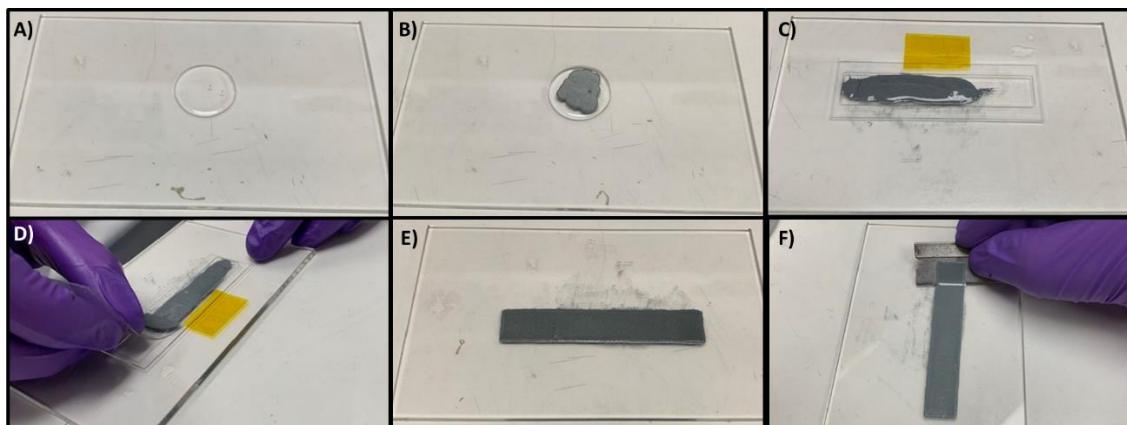


Figure 14: A schematic revealing the process of fabricating AM:PDMS thin films. PDMS is measured onto a glass pane (A), AM is measured on weigh paper and poured over PDMS and mixed (B), a PETG mask is applied (C), the sample is spread across the well (D), the mask is removed and the glass pane is placed in an oven to cure (E), the film is removed with a straight razor

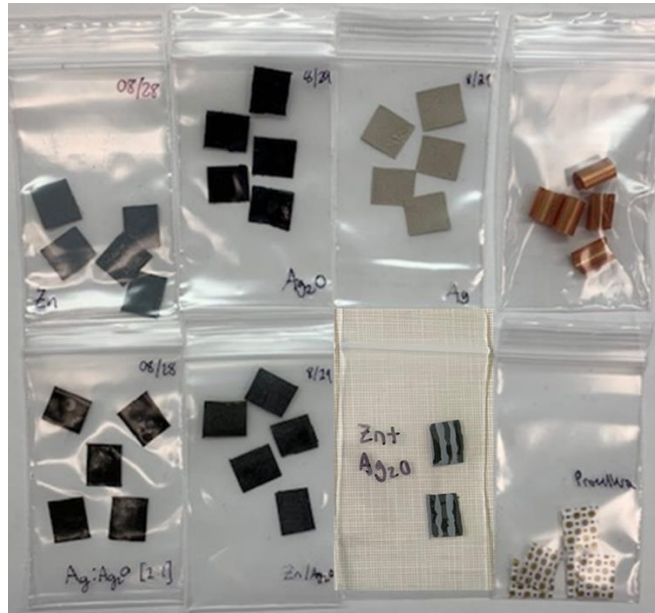


Figure 15: A photo showing composite films (left to right, top to bottom) Zn, Ag, Ag₂O, Ag-coated catheter, Ag/Ag₂O, Zn/Ag₂O mixed, Zn/Ag₂O striped, and a bio electric dressing

3.4 Fabrication of Coated Catheter Prototypes

Preparing a complete Foley catheter adds many more technical challenges. A two-piece mold must be prepared to form the main body of the catheter including two lumens/ports for flushing urine and inflating the balloon. One-way valves must be added to the proximal balloon port using a medical grade adhesive. Finally, a balloon must be adhered to the distal end of the catheter. It is also very likely that the ratio of active materials to polymer becomes so high that the material becomes too costly to manufacture and starts losing its mechanical toughness. For this purpose, the process shown in Figure 16 is proposed. A mold (Figure 16A), is coated in a thin layer of high ratio paste and partially cured (Figure 16B). Then additional pure PDMS can be poured/injected into the bulk of the mold (Figure 16 C), and the cured in one piece or two bondable pieces (Figure 16 D), resulting in the final product (Figure 16 E). This method focuses the active materials to the surface of the catheter while allowing the bulk of the catheter to be made without the cost of active materials.

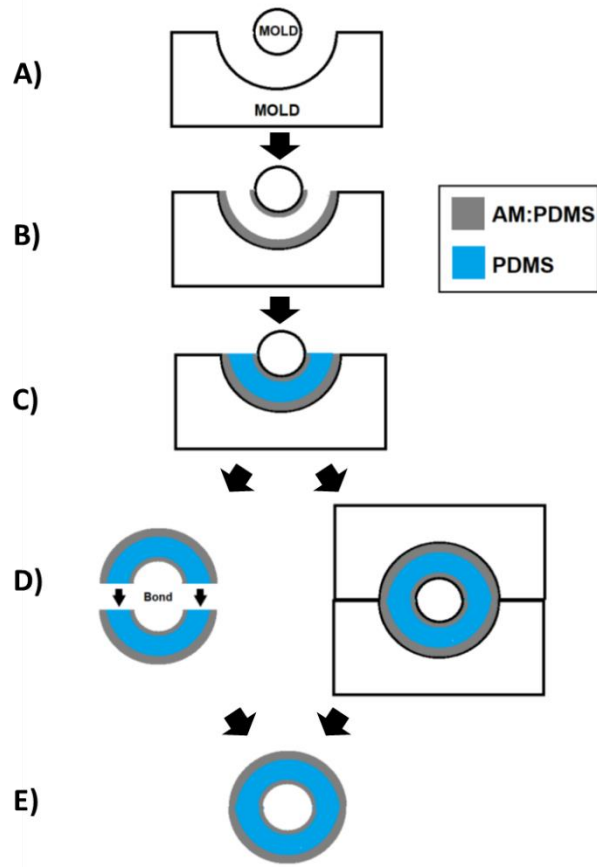


Figure 16: A schematic revealing the use of a mold to maintain AM at the surface of the catheter.

The two-piece method shown in Figure 16 was employed to fabricate a prototype, balloon-free, distal end of a catheter. The molds were machined from aluminum using a 7 mm ball end mill. A 2 mm hole is drilled at the distal tip to support one end of the 2 mm lumen mold, while the other end is supported by the wall of the mold. An image of the mold can be seen in Figure 17. After the AM:PDMS pastes are prepared, the molds are heated in an oven at 125C for 2 minutes. This allows the curing process to begin as the pastes are painted on to the inner surfaces of the mold. The lumen mold is positioned, pure PDMS is added to fill the rest of the space in the mold, and finally, the filled molds are cured in an oven at 125C for 15 minutes. Each half of the cured catheter is carefully removed from the molds and adhered to one another using a silicone-based adhesive (Sil-Poxy™ Smooth-On, Inc.). The distal flush ports

(sometimes referred to as eyes) are cut/punched using a sharp blade/punch. Following preparation, AM:PDMS pastes can also be coated directly onto a commercial urinary catheter and thermally cured. In addition to the molded catheter, sections of a commercially available silicone catheter were coated by spinning each section along the luminal axis, and painting on the AM:PDMS pastes. The sections are cured with a heat-gun while spinning to allow for uniform coating thickness. The results of each method, respectively, are shown in Figure 18.

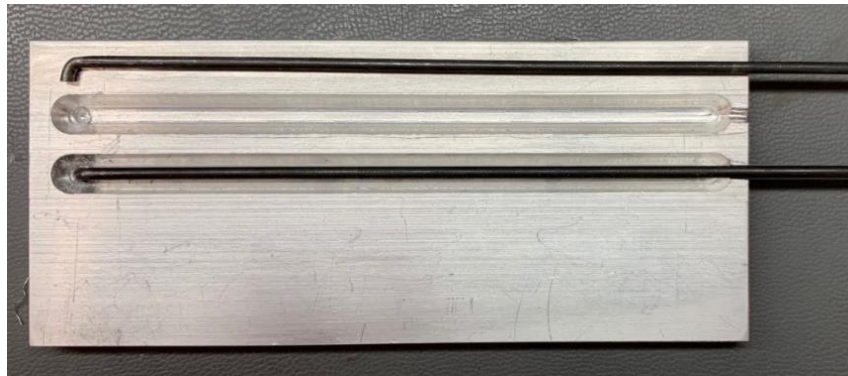


Figure 17: A simple machined aluminum mold and two steel lumen-molds

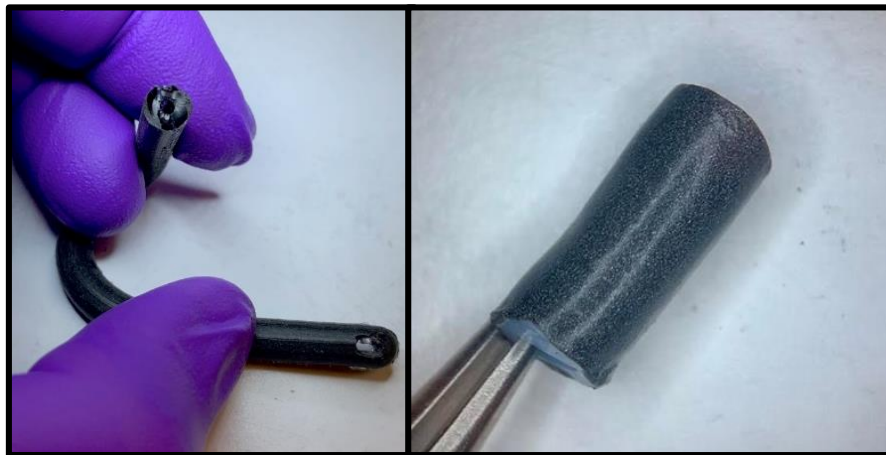


Figure 18: Photo displaying the final (balloon-free) single lumen Ag/Ag₂O:PDMS catheter (left) and a section of commercially available coated in Zn/Ag₂O:PDMS (right)

Chapter 4: Experimental Methods

In this Chapter, the methods used to test the reactivity and the strength of biofilm inhibiting effects of prepared coatings are described.

Synthetic Urine

The synthetic urine was prepared by combining reagents found in Table 8 [61], and filtering through a 0.2 μ m filter.

Table 7: A simple recipe for the growth of urinary pathogens [61]

Component	Quantity (g)	Concentration (mmol/L)
Peptone L37	1	
Yeast Extract	0.005	
Lactic Acid	0.1	1.1
Citric Acid	0.4	2.0
Sodium bicarbonate	2.1	25
Urea	10.0	170
Uric acid	0.07	0.4
Creatinine	0.8	7.0
Calcium chloride·2H ₂ O	0.37	2.5
Sodium chloride	5.2	90
Iron (II) sulfate·7H ₂ O	0.0012	0.005
Magnesium sulfate·7H ₂ O	0.49	2.0
Sodium sulphate·10H ₂ O	3.2	10
Potassium dihydrogen phosphate	0.95	7.0
Di-potassium hydrogen phosphate	1.2	7.0
Ammonium chloride	1.3	25
Distilled water	To 1 Liter	

Open Circuit Cell Potential Measurements

A standard electrochemical setup with a high impedance electrometer was used to determine the open circuit potential of silver foil relative to zinc foil at room temperature in atmospheric conditions. Synthetic urine was used as the electrolyte for one experiment and DI water for the other. Additionally, there was no mixing or disturbance to the media during measurement.

Peroxide and pH Measurement

In order to explore the quantity of hydrogen peroxide produced by the samples containing the active materials being studied, replicates ($n = 3$) of Zn:PDMS, Ag:PDMS, Ag₂O:PDMS, Ag/Ag₂O:PDMS, Zn/Ag₂O:PDMS, and striped Zn and Ag₂O:PDMS were tested. The weight of each sample was recorded. Samples were sterilized with 100% Ethanol and left to dry in the bottom of glass containers overnight. While working under a flame, 1.5mL of synthetic urine (pH = 7) was injected onto the glass containers. At each time point, 20 μ L of synthetic urine were removed from each sample container and placed directly on the tile of either Quantofix 25 or Quantofix 100 peroxide strips to reveal a color change quantified by comparison to a colorimetric scale. The Quantofix 25 concentration scale measures: 0, 0.5, 2, 5, 10, and 25 mg/L. The Quantofix 100 concentration scale measures: 0, 1, 3, 10, 30, and 100 mg/L. The pH of the urine was measured with litmus paper before being separated into the glass containers and for all samples following the thirteenth (last) day.

Goniometry

To determine the wettability of the samples, Sessile drop, contact angle goniometry was performed. The samples were placed under a Keyence VHX 1000 video microscope, positioned at 90 degrees. A 2 μ L drop of pure DI water was pipetted onto the five separate edges of each sample. The angle is measured using the line and angle measurement tools. Testing was performed on pure PDMS as well as samples made with PDMS mixed with Ag₂O, Ag, Ag/Ag₂O, and Zn/Ag₂O.

Antimicrobial Resistance

A 48-hour ($n = 2$) and 144-hour ($n = 5$) antimicrobial resistance study was performed to compare the short-term and long-term effectiveness of selected antimicrobial samples. The samples for the short-term study included: PDMS, Ag:PDMS, Zn:PDMS, Ag/Ag₂O:PDMS, Zn/Ag₂O:PDMS, Zn and Ag₂O patterned :PDMS, and sections of a commercially available “silver-coated” catheter. The samples for the long term study included: PDMS, Ag:PDMS, Zn:PDMS, Ag/Ag₂O:PDMS, Zn/Ag₂O:PDMS, Ag₂O:PDMS, a bioelectric dressing (Procellera®), and sections of a commercially available “silver-

coated” catheter (Cardinal Health). The control for the bio electric dressing was a polyester woven cloth. The control for the AM:PDMS was pure PDMS. There was no control for the “silver coated” catheter. Positive controls for absorbance measurements are test tubes containing only urine and the inoculum. Negative controls for absorbance measurements are test tubes containing only urine without inoculum. In addition to composite films, a standard, commercially available 100% silicone catheter was cut into equal size sections having similar surface area to composite films. The outside of the catheter sections were coated with Zn/Ag₂O:PDMS or Ag/Ag₂O:PDMS or nothing and subject to the 144-hour (6-day) biofilm study.

All composite films were cut into squares with a face area of 168 mm² (12mm X 14mm). All samples, apart from the bioelectric dressing and its control, were washed with 100% ethanol and placed at the bottom of a test tube to dry for overnight. Procellera and its control were sterilized under UV light for 8 hours on each side and placed into individual test tubes. The sample-containing test tubes are filled with 3 mL of synthetic urine [61] and inoculated with *E. coli* (BW 25113) to a known optical density (OD₆₀₀ = 0.01). At regular intervals, a 20 µL volume is taken from each sample container and placed in a cuvette for measuring the absorbance of light (600nm) using a spectrophotometer (BIORAD SmartSpec™ 3000). To facilitate growth, the tubes were placed in an incubator at 37C without shaking. For the 144-hour study, every 48 hours the samples were placed removed from their current test tubes and placed into new test tubes with 3 mL fresh synthetic urine, and re-inoculated with bacteria to OD₆₀₀ = 0.01. This set up intended to simulate the environment that would be present in a urethra. At the end of each study, all samples were placed into sterile glass test tubes full of 3 mL of distilled water, to stunt further growth. To shed biofilm from the samples into solution for quantification, we place the test tubes in an ultrasonic bath (Branson Ultrasonics CPX Series M 1800) at maximum frequency for three, thirty second intervals, ten seconds apart [20]. A serial dilution was performed until colonies are quantifiable on LB agar plates incubated at 37C for 24 hours.

Zone of inhibition studies are a common practice for researchers and pathology labs for testing resistance to antibiotics. The AM:PDMS films are cut into 8 mm diameter discs using a biopsy tissue punching device. Bacteria are cultured for 24 hours in synthetic urine and coated onto LB agar plates. Disks are placed in the center of agar, and plates are incubated overnight at 37C. Radii of zones of inhibition are measured from center of disk to the edge of bacterial lawn.

Statistics

Data is plotted using means and standard deviations. The Welch's t-test is used to test the hypothesis that the AM:PDMS coatings are more effective at inhibiting biofilm than just PDMS (placebo) using a confidence interval of 95%.

Chapter 5: Experimental Results

5.1 Open Circuit Cell Potential Measurements

The measured open circuit potential of silver foil vs. zinc foil in water and in urine, shown in Figure 19, have different profiles over the span of 360 minutes. Initially, the open circuit cell potentials in both media show variations. The variations may be associated with the occurrence of different reaction equilibriums. Following the period of variation, the open circuit potential in DI water rises, appearing to approach a plateau around 1.2 volts. The rise and plateau signify the overall reaction taking place at the surface is approaching and maintaining a stable equilibrium. The initial variation of open circuit potential before a stable equilibrium is maintained takes less time in synthetic urine. Additionally, the potential during the period of stable equilibrium is roughly 0.97 volts, which is -0.25 volts less than in water, but implies that the passive redox reaction is possible in urine and supplies a potential of roughly 0.97 volts.

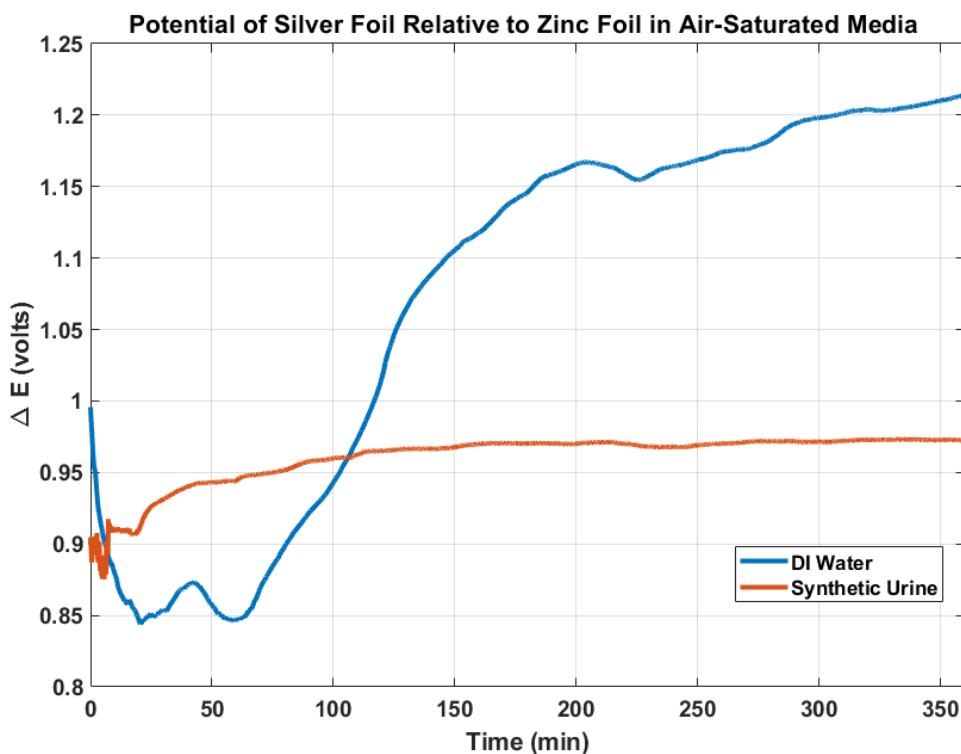
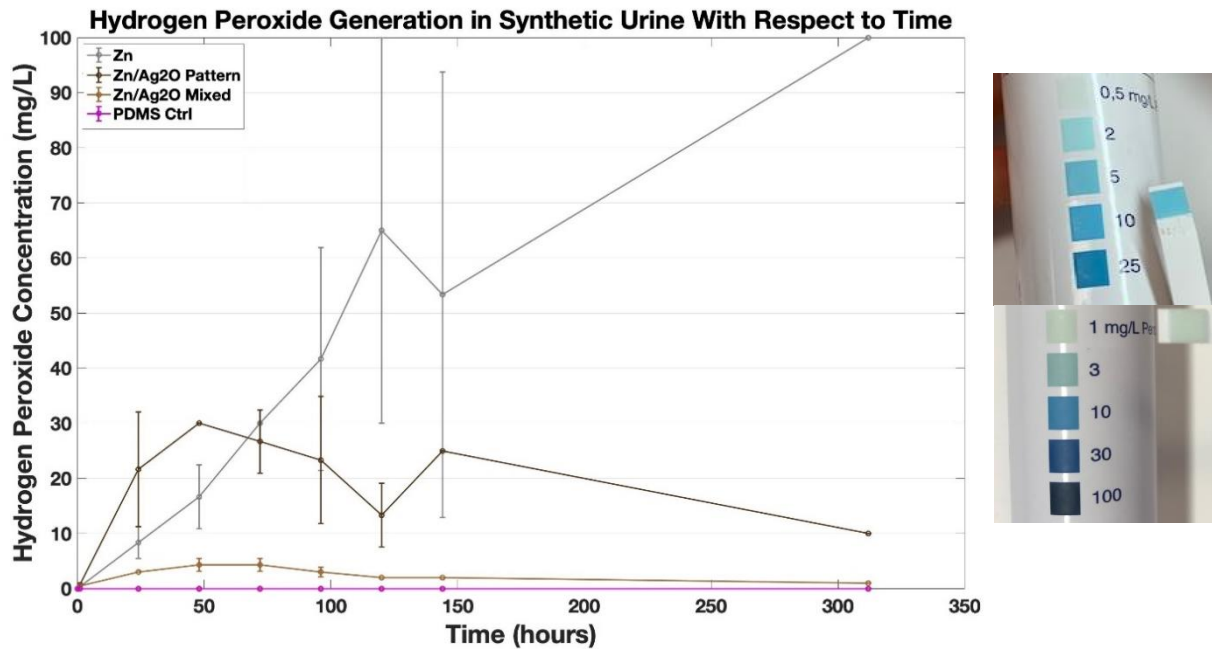


Figure 19: A plot of potential difference with respect to time. The potentials of silver foil relative to zinc foil in Air saturated synthetic urine and DI water are similar

5.2 Hydrogen Peroxide and pH Measurements

The plot in Figure 20 shows the concentration of hydrogen peroxide measured over the course of thirteen days. The images to the right of the plot confirm the resolution of the colorimetric scale, which also accounts for the size of certain error bars seen in the plot. Only samples containing zinc contributed to generation of hydrogen peroxide in the urine. All other samples were unable to generate enough hydrogen peroxide to be within the detection limits (< 0.5 mg/L) and were omitted from the plot with the exception of the PDMS control. Both samples containing a mix of zinc and silver oxide, generated less hydrogen peroxide than samples with zinc alone. However, the samples made with a striped pattern produced more hydrogen peroxide, as opposed to the samples that were mixed.



Time (days)	(-) Ctrl	PDMS Ctrl	Zn A	Zn B	Zn C	Ag A	Ag B	Ag C	Ag ₂ O A	Ag ₂ O B	Ag ₂ O C	Ag/Ag ₂ O A	Ag/Ag ₂ O B	Ag/Ag ₂ O C	Zn/Ag ₂ O A	Zn/Ag ₂ O B	Zn/Ag ₂ O C	Zn+Ag ₂ O A	Zn+Ag ₂ O B	Zn+Ag ₂ O C
0	7	7	7	7	7	7	7	7	7	7	7	7	7	7	7	7	7	7	7	7
13	7	7	7.5	8	7	7	7	7	7.5	8	8	7.5	8	8.5	7.5	8	7.5	8	8	8

Figure 20: Shows the concentration of hydrogen peroxide measured with respect to time (top-left) using either test scale (top-right). The synthetic urine increased alkalinity for samples containing zinc or silver oxide after a period of 13 days (bottom)

The bottom of Figure 20 shows the pH before and after the thirteen-day period. The pH of the synthetic urine showed increases for samples containing zinc and/or silver oxide. There were no pH changes in the urine containing the silver composites, which is likely do to the absence of a strong reducing agent or a strong oxidizing agent (zinc and silver oxide, respectively). The pH changes are consistent with the occurrence of various redox reactions occurring at the surface.

5.3 Microscopy of a Zn/Ag₂O:PDMS Composite Film

Figure 21 shows microscope images of a Zn/Ag₂O composite that had been kept dry and one that had been submerged in synthetic urine for twenty-four hours (seen within the yellow boundaries). The images present visual evidence of passivation layers building on Zn/Ag₂O:PDMS samples after they were exposed to urine. Initially, these samples could be described as a homogenous spectrum of black and gray specs (before). After twenty-four hours, a white build-up began to form on the surfaces of each sample (after). Scratching away the white build-up (red circle) from within the boundaries of the blue box in Figure 21A revealed a brown hue beneath, as depicted by the red box in Figure 21C. Higher magnification images of the composite films before and after the passivation layer is removed can be seen in Figure 21 B and C, respectively. It is possible that chloride ions in the urine are reacting with the silver to form silver chloride. It is also possible that zinc is forming zinc hydroxide, see equation 5'. Both products appear as a white crystalline build-up. However, moistened silver chloride has been known to decompose when exposed to light, turning brown in color [62]. This may explain the brown pigment visible on the surface of the sample. On the other hand, it is possible that the silver ions are reacting with phosphate or sulfate ions found in the urine; both silver phosphate and silver sulfate appear brown in color.

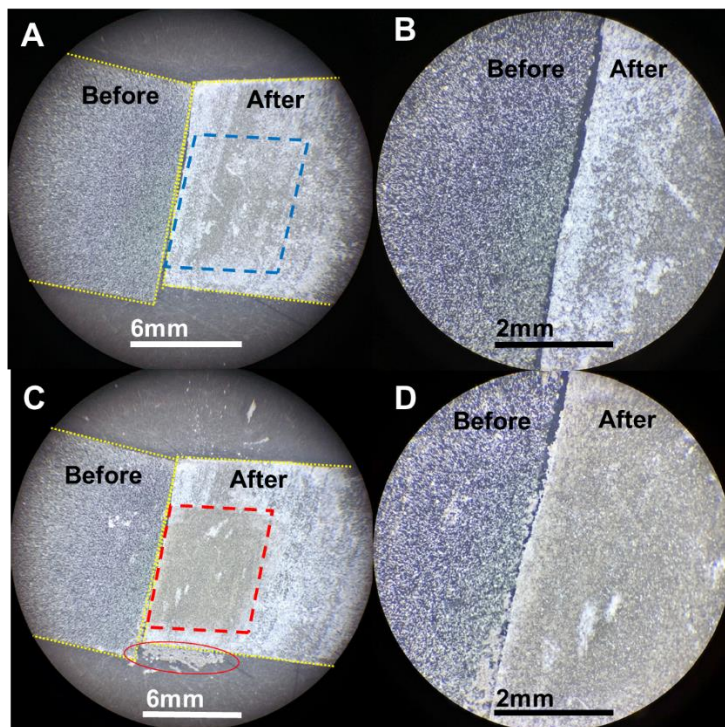


Figure 21: A Zn/Ag₂O:PDMS composite before and after (right and left, respectively) being exposed to urine following twenty-four hours in synthetic urine. A white crystal residue formed on the surface (A, B). Beneath the residue a brown discoloration is visible (C, D)

5.4 Goniometry

The bar chart in Figure 22 shows the mean and standard deviation for contact angles of 2 μ L water droplets on each composite and a control (PDMS). Figure 22 A and B are single measurements taken of PDMS and Zn/Ag₂O:PDMS films, respectively. The bars chart shows a quantifiable difference in surface wettability following addition of the active materials. Compared to the pure PDMS surface, all composite samples are more hydrophilic ($n = 5$, $p < 0.05$). Based on the standard deviations, it is difficult to say which composite is more or less wettable, only that they are less than the control. The hydrophilicity is welcomed as it has been shown to resist bacteria adhesion. However, because all samples form water drop contact angles that are greater or equal to 90 degrees, they are all still considered to be slightly hydrophobic or have low wettability.

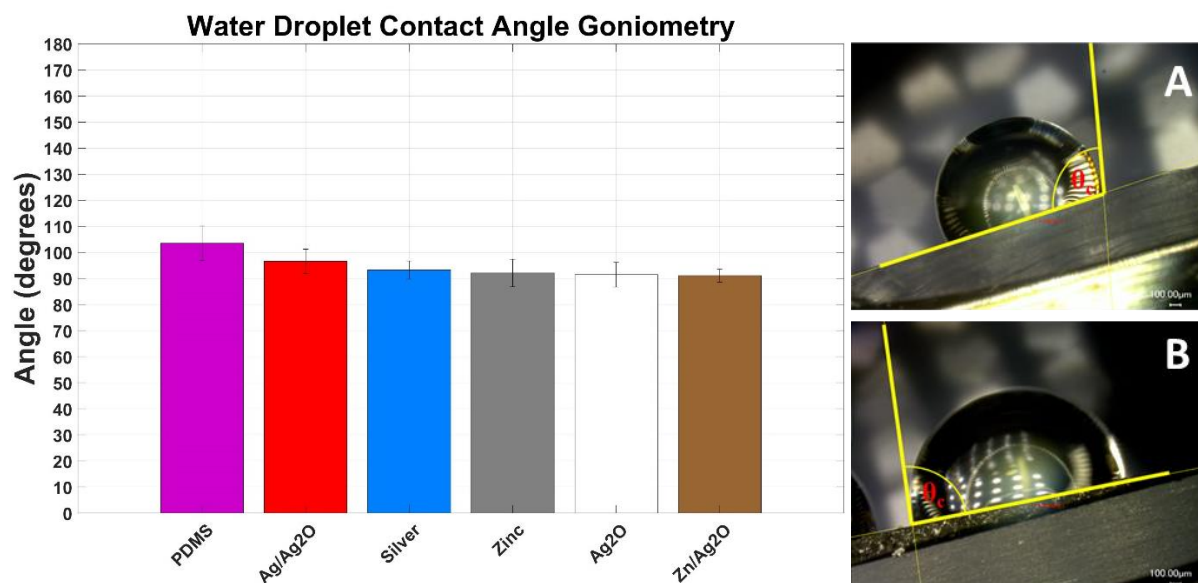


Figure 22: A bar chart showing contact angles measured for AM:PDMS composites accompanied by images of the contact angle formed on a PDMS (A) and Zn/Ag₂O:PDMS film (B).

5.5 Antimicrobial Resistance Measurements

It is possible to track the growth of planktonic bacteria in solution using spectrophotometry. The absorbance of light (600nm) emitted by the machine was measured when passing through a cuvette containing an aliquot of the media containing the inoculum. The optical density increases as more light is absorbed by colloid in solution. The sigmoidal curves apparent in Figure 23 are consistent with that of bacterial growth. Following the first lag cycle, we see rampant growth in PDMS, striped Zn/Ag₂O:PDMS, and Zn:PDMS. The commercially available “silver-coated” catheter is inhibiting growth only slightly, but not as much as the samples prepared in the lab. Among them, the Ag:PDMS had strong antimicrobial effects in solution. This is puzzling as elemental silver is less likely to release silver ions into solution.

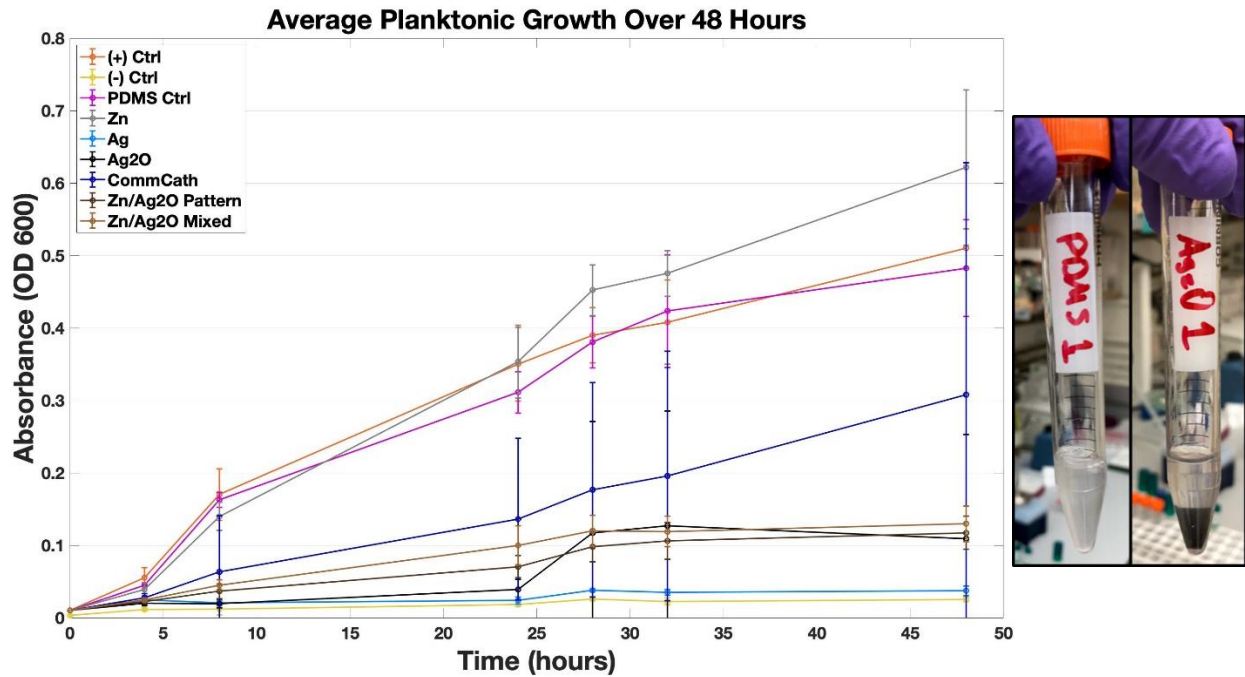


Figure 23: A plot of absorbance OD₆₀₀ with respect to time for selected samples (left). A photo of a pure PDMS and Ag₂O:PDMS samples in inoculated synthetic urine (right). The more bacteria in solution the higher the absorbance

The biofilm shed from samples via ultrasonic bath can be quantified by counting the number of colony forming units that grow from a known volume of solution onto LB agar plates. The number of colonies that form on the plates are counted and used to calculate a concentration using units, CFU/mL. A greater number of colony forming units per milliliter corresponds to a higher number of bacteria growing on the surfaces of the sample. It should be noted that the axis for CFU/mL is logarithmic. We can see in Figure 24 that samples containing zinc had a positive effect on the bacteria, allowing them to grow on the surface. Samples with silver, including the commercial catheter, seemed to perform better for a 48-hour study. When comparing final absorbance magnitudes to the number of CFU/mL, a paradigm is revealed where planktonic bacteria and biofilm are affected independently. For example, the silver catheter inhibits the growth of bacteria moderately within forty-eight hours, but does exceptionally well inhibiting biofilm. The opposite is seen for samples combining zinc and silver oxide. It is difficult to compare samples that equally inhibit bacterial growth, which is why a study lasting up to a week was proposed.

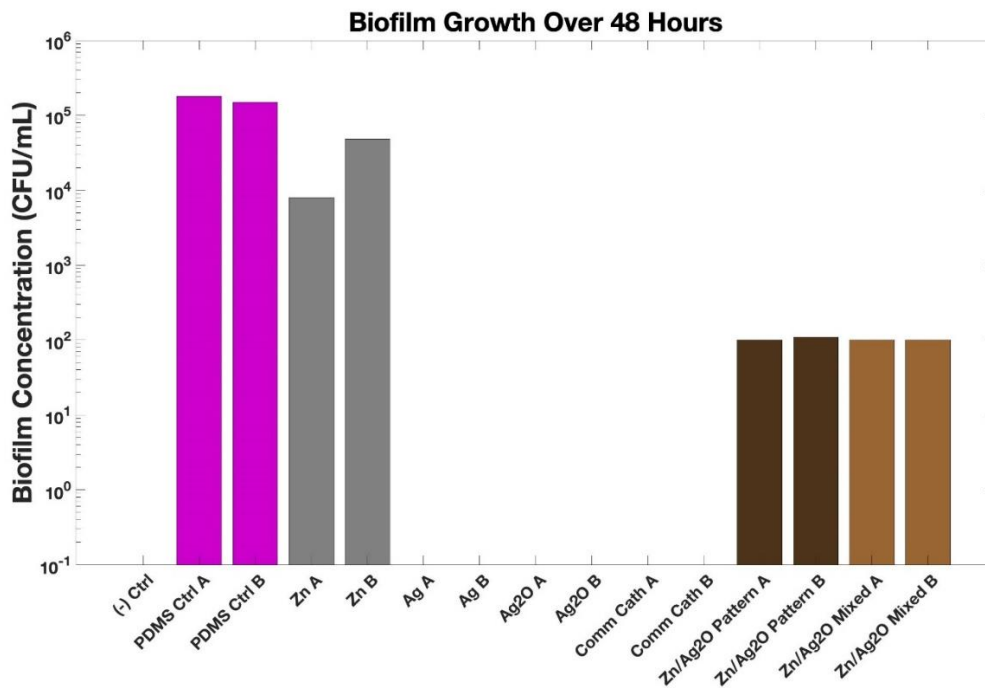


Figure 24: A plot of biofilm concentration in CFU/mL growing on the surface of selected samples following 48 hours. Samples with higher concentrations perform worse in inhibiting biofilm

The six-day study shown in Figure 25 is broken into three 48-hour intervals. Following a 48-hour interval, bacteria in the synthetic urine reach a lag cycle. At this point in time most of the nutrients available to the remaining bacteria in solution are gone. The bacteria become affected by increasing concentrations of their own metabolic byproducts. These harsh conditions can force gene mutations and cell death. For this reason, following a period of forty-eight hours, the synthetic urine is refreshed. This also mimics the bladder as urine is constantly being produced and flushed out of the bladder. Physiologically, the refreshed urine in a urinary tract is expected to still have small concentrations of bacteria present while a patient is catheterized [26]. As mentioned previously, the mechanism by which bacteria are being inhibited are complex and can affect growth in solution and on surfaces independently. The study was terminated following 144 hours, as the absorbance of well performing samples approached the magnitude of the controls.

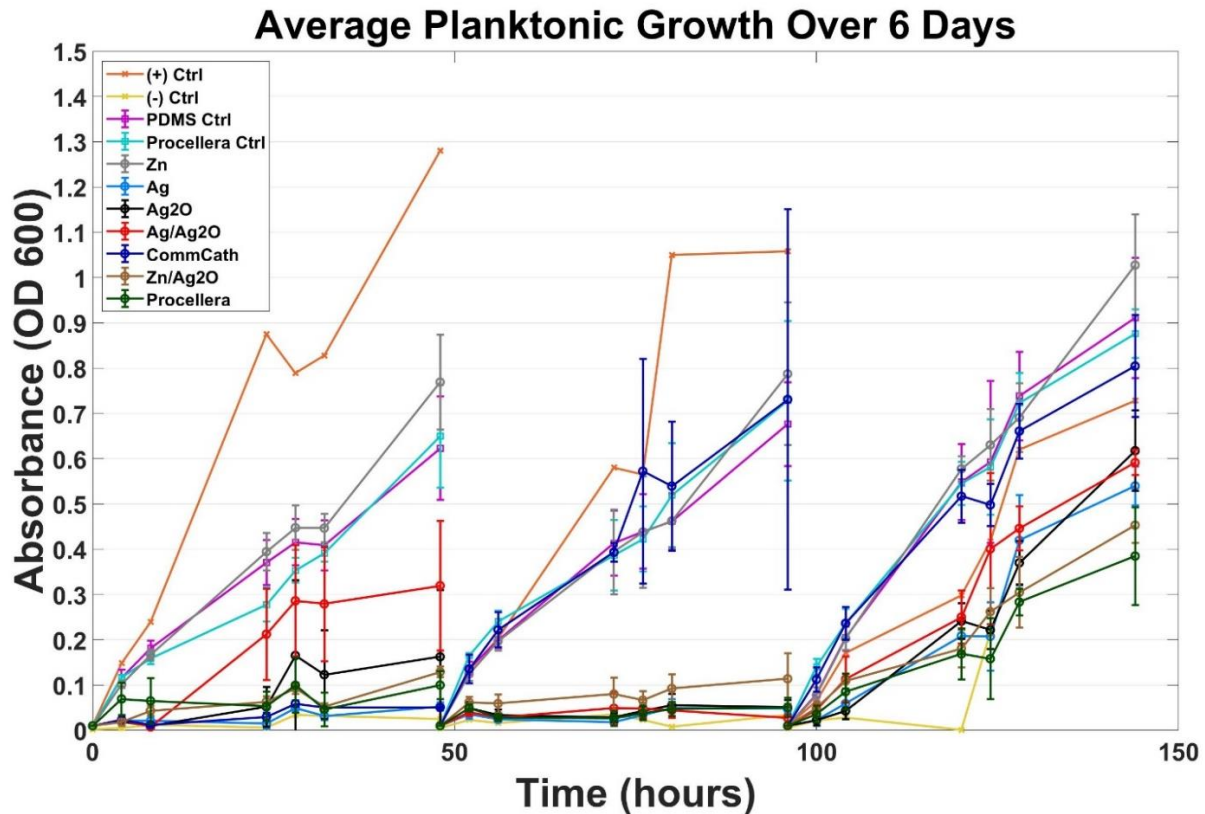


Figure 25: A plot of absorbance OD₆₀₀ with respect to time for selected samples over a 6-day period

The growth curves following each 48-hour cycle in Figure 25 shows unique differences from sample to sample. Across the six days, the positive control showed uncontrolled growth and the negative control started to show growth following 120 hours. Fortunately, the contamination of the positive control occurred hours after the remaining samples started growing. The PDMS sample, the Procellera control, and the Zn:PDMS also showed strong growth of *E. coli* in solution across six days. During the first forty-eight hours, Ag/Ag₂O:PDMS allowed more growth than the remaining samples. After the forty-eight hours, the Ag/Ag₂O:PDMS began to inhibit bacterial growth comparable to the remaining samples, except for the commercially available catheter. It is possible that the commercial silver catheter does have a coating of soluble silver, however, after the urine is refreshed, it appears that there is not enough left to continue inhibiting growth in solution. Not until after the second 48-hour cycle do bacteria become resistant across all samples. It is unclear at what time between forty-eight hours and ninety-six hours the

samples actually begin to lose effect. This is because the E. coli may have all died upon exposure to the films at the start of the second 48-hour cycle, and no further inoculation occurs until hours later. It may be a good idea to inoculate and refresh synthetic urine every twenty-four hours in future experiments.

Biofilm was quantified from all samples following repeated exposure to fresh urine and E. coli over six days. The results are shown in Figure 26. A higher concentration of CFU/mL is proportional to a higher concentration of biofilm. Compared to the pure PDMS, Ag:PDMS, Ag₂O:PDMS and Ag/Ag₂O:PDMS were at least five orders of magnitude lower in biofilm (p-value < 0.05). The bioelectric dressing performed slightly worse (p < 0.01). The commercial catheter and Zn:PDMS were both ineffective at inhibiting biofilm (p < 0.05). Although Zn/Ag₂O:PDMS showed antimicrobial effects in solution, it did not completely prevent biofilm formation. Except for the commercial catheter, samples containing silver are associated with lower concentrations of bacteria. It is possible that the E. coli are using zinc as a nutrient, while silver ions may be the main mechanism behind biofilm inhibition.

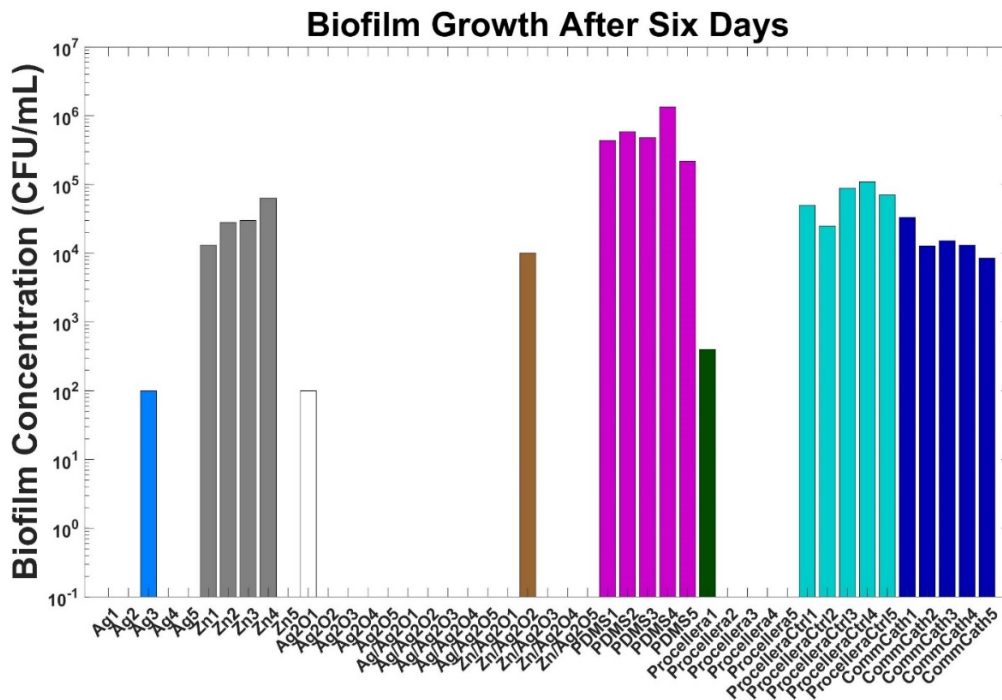


Figure 26: A plot of biofilm concentration in CFU/mL growing on the surface of selected samples following six days. Samples with higher concentrations perform worse in inhibiting biofilm

The results in Figure 27 give further insight into the mechanism acting to inhibit bacteria. If bacteria are growing anywhere on the disk ($R < 4$ mm), then the sample was unable to inhibit growth. If a zone of inhibition appears at the edge of the disk ($R \approx 4$ mm), then the sample is capable of inhibiting growth about its own surface area. Finally, when a zone of inhibition appears beyond the edge of the disk ($R > 4$ mm), then it suggests that the disk generates a product that can diffuse freely into the agar. What is clearer from these results is the effect of using a reducible form of silver and/or a strong redox couple. Samples containing only silver (I) oxide had variation in how large of a zone was inhibited. Following incorporation of pure silver powder or zinc powder, the diffusive killing affect is much more dramatic. Samples were able to inhibit *E. coli* up to 9mm away from the edge of the disk. This suggests that these particular films have an improved delivery of a diffusive antimicrobial mechanism.

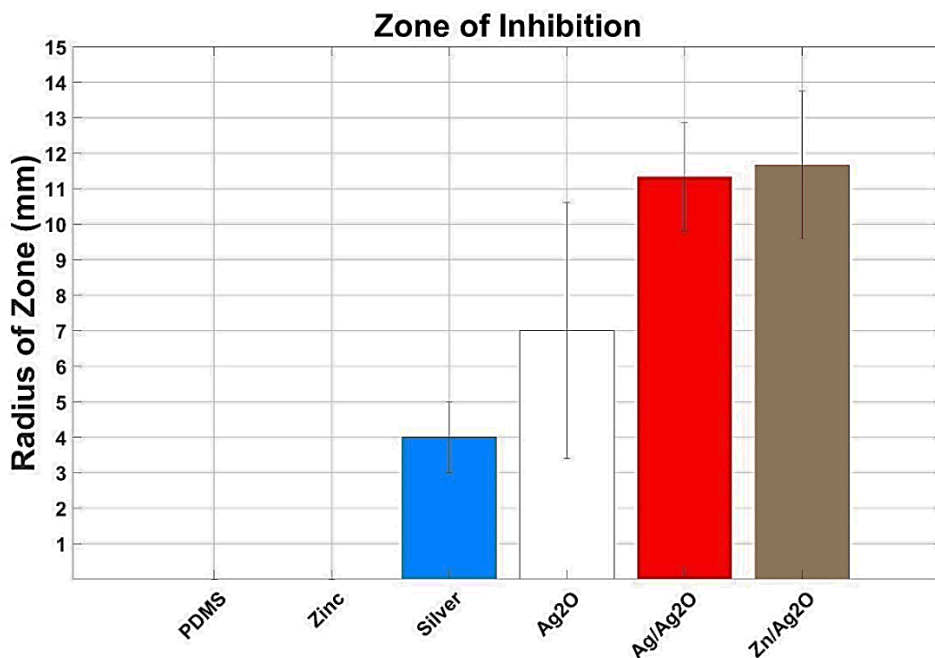


Figure 27: Zone of inhibited bacteria about the 8mm disk of AM:PDMS films on LB agar plates coated with *E. coli* (n=3). Radius of zone is measured from center of disk

The two best performing composites formulations were selected and used to coat sections of a standard, commercially available, silicon urinary catheter. A comparison of the biofilm inhibiting effects, shown in Figure 28, demonstrates that the Ag/Ag₂O:PDMS coatings created a four order of magnitude reduction in the concentration of biofilm compared to controls ($p < 0.05$). The Zn/Ag₂O:PDMS coatings created a five order of magnitude reduction in the concentration of biofilm compared to the controls ($p < 0.05$). This difference may suggest that the Zn/Ag₂O:PDMS has additional effects. These effects may be electricidal or possibly an improvement in the release of silver ions.

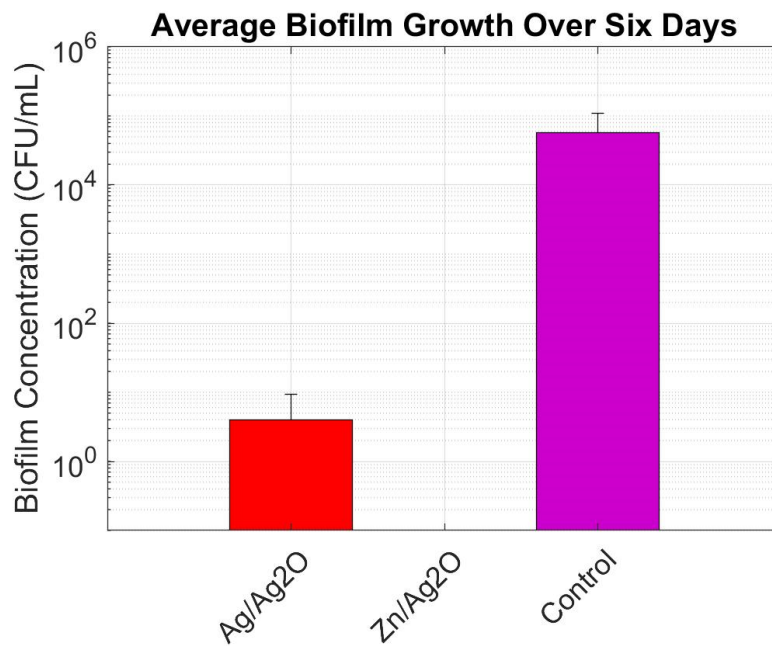


Figure 28: Biofilm concentrations measured from catheter sections coated with antimicrobial composites following six days (n=5). Samples with higher concentrations perform worse in inhibiting biofilm.

Chapter 6: Discussion of Experimental Results

6.1 Discussion

A number of experimental techniques were used to characterize the effects generated by the composite films in solution. The open circuit cell potential measurements provided a means to compare the zinc-silver model in DI water and urine. Quantifying the concentration of hydrogen peroxide and changes in pH in the bulk solution following exposure to the composite films gives insight on electrochemically associated reactions. Observation of any changes of surface characteristics and quantification of surface wettability is additionally valuable to the study. Finally, subjecting sections of composite films and similar medical devices to urine inoculated with *E. coli* is the ultimate test to determine if the composites are indeed antibacterial.

The open circuit cell potential measurements show variations, during the initial portion of the time scale. This agrees with measurements taken by Banerjee et al. [19]. However, Banerjee et al. terminated the measurement at 100 minutes. In DI water, the cell potential starts approaching a stable equilibrium after sixty minutes. In urine, the cell potential has similar variations, but reaches a stable equilibrium at 0.97 volts. Based on the Nernst equation, the stable open circuit potentials in each media are consistent with micromolar concentrations of aqueous silver and zinc at the electrode surface. These potentials are also consistent with the electric fields at the surface. It can be concluded that a passive redox reaction between zinc and silver may be formed in urine, assuming it contains some dissolved oxygen.

Concentrations of hydrogen peroxide were detected only in samples containing zinc. Although the minimum detection limit of hydrogen peroxide is 14.7 μM in the bulk of the urine specimen, concentrations may be higher at the surface of composite. Decreasing the amount of zinc in the composite resulted in a decrease in the concentration of hydrogen peroxide. These results agree with the hypothesis in Chapter 2 that zinc by itself is able to generate hydrogen peroxide by the reduction of soluble oxygen.

Similarly, the pH local to the surface can vary greatly from the bulk of the urine. The alkalinity formed by composites containing zinc and/or silver oxide also suggest redox reaction conditions. This notion is further validated by physical changes in color and crystallization revealed by microscopic inspection of the composites following long term exposure to urine.

Two very conclusive results were obtained from the results of the antimicrobial resistance tests. First, films solely containing zinc were unable to reduce the concentration of planktonic bacteria and biofilm. It is possible that the bacteria were using the zinc as a source of nutrition or to help catalyze other cellular processes. Second, samples containing reducible forms of silver performed well in inhibiting *E. coli*. More important than elemental silver is a reducible form of silver, such as silver oxide or silver chloride. These have the ability to react with oxygen, hydroxide, and other ions in solution to free silver ions into solution. It is understood that silver ions are extremely toxic to bacteria. The elemental silver used to make the composites may have a thin layer of oxide, similar to the zinc, that may have initially contributed to release of silver ions in solution. But it is very likely that silver oxide containing samples allowed reduction reactions to increase in number or perpetuate for longer durations of time. It would be of great interest to study how varying the amounts of elemental silver and silver oxide in a sample could do this.

Adding the zinc to the silver oxide had mixed effects. In the 48-hour study the zinc and silver oxide samples were able to inhibit bacterial growth in solution, but not as much on the surface, compared to the commercial silver coated catheter and the samples containing exclusively silver or silver oxide. The 48-hour study and the six-day study show similar results for zinc mixed with silver oxide, which inhibited planktonic bacteria. However, these samples showed less biofilm after six days. The bio electric wound dressing performed as well as any of the silver-containing composites. When taking into account only the absorbance and biofilm concentration plots, it is very difficult to determine which composite works the best at inhibiting growth of bacteria. It appears as though any sample containing silver is comparable. The zone of inhibition study suggests that the combination silver or zinc with silver oxide creates a greater

zone, corresponding to greater diffusion of a biocidal agent. This agent is most likely silver ions. It is possible that hydrogen peroxide is formed when including the zinc. However, the highest concentration of hydrogen peroxide measured was 100 mg/mL or 2.94 mM using only zinc, which was not effective against the planktonic or biofilm *E. coli*. This is consistent with the idea even non-virulent strains of bacteria are capable of protecting themselves from hydrogen peroxide and peroxide anions[40].

Given the fact that the Zn/Ag₂O:PDMS films did as well as the Ag/Ag₂O:PDMS films, it is difficult to suggest that the e-fields and microcurrents formed between zinc and silver particles on the surface are significant enough to inhibit biofilm. However, the results from using coated catheter sections in the six-day study, showed a slight increase in the reduction of biofilm concentration for the Zn/Ag₂O:PDMS coating (one order of magnitude). This may point to electricidal effects at work. To build a better electrochemical reaction, the amounts of zinc and silver could be varied. Additionally, a combination of all three powders has yet to be investigated. Alternatively, it may be useful to further investigate alternate patterns of zinc and silver oxide to enhance electricidal effects. The strength of the electric fields can be influenced by the proximity of the individual zinc and silver oxide particles because the magnitude of the electric field by definition (V/m) is influenced by the separation of the electrodes. Therefore, changes in the resulting e-field should affect the antimicrobial results. Furthermore, the mean particle sizes for the zinc, silver and silver oxide powders were not uniform. Further investigations may benefit from restricting variations in particle size of all active material species.

Comparatively speaking, the methods developed in the lab to create antimicrobial coatings may be better than those used to make the commercial silver catheter. As previously mentioned, one of the greater difficulties of this project is localizing the active materials at the surface of the catheter, instead of inside of it. The commercial “silver” catheter is advertised as a silver phosphate catheter coupled with a hydrogel coating. The bioelectric wound dressing uses a patterned zinc-silver coating. These two products are examples of how silver can be used in different ways to produce similar effects. Also, these effects are not exclusive to one type; synergistic approaches (e.g. silver *with* hydrogel) are becoming more popular in

preventing biofilm. It would be interesting to compare the Ag/Ag₂O:PDMS and the Zn/Ag₂O:PDMS coatings with additional commercially available antimicrobial catheter options.

One fortunate observation is that, in addition to greatly reducing the concentration of biofilm, the Ag/Ag₂O:PDMS and the Zn/Ag₂O:PDMS coatings were strongly adhered to the catheter substrates. More testing should be done to measure the strength of adhesion on catheter substrates. Additionally, it would be valuable to test the adhesion of these coatings on other substrates used for devices with similar antimicrobial needs, e.g., esophageal nitinol stents, gastronomy tubes, and others.

Chapter 7: Conclusion

The novelty of each coating method lies in the ability to have a minimal amount of active materials at the surface of the catheters such that it perpetuates antimicrobial reactions only when in contact with fluids. All of the evidence suggests that this objective has been achieved. The coating must perpetuate the reactions for a minimum expected duration of time before replacement. Antimicrobial reactions over a period of six days has been achieved thus far. This coating may be applied to any medical device that is intended to dwell in the body for a short period of time (1-30 days). The method for coating is novel in the sense that it can be optimized to maximize adhesion to other substrates and maximize antimicrobial effects following deployment. This may greatly add value to both patients and hospitals when combating incidences of infection.

Further research into methods to controllably release silver ions from surfaces of medical devices like urinary catheters or esophageal stents should be continued. The evidence currently supports the assumption that silver is more important than peroxide or e-fields. E-fields in the immediate vicinity may play a role, but these phenomena were not able to be measured. Since there may still be a ratio of anodic and cathodic active materials capable of generating antimicrobial e-fields or microcurrents, research in varying these ingredients would also be very valuable. It may be more effective to coat medical devices with thin (100-200 μm wide) concentric, alternating rings of the Ag/Ag₂O:PDMS and Zn:PDMS; other

patterns maybe more effective at silver release and electricidal effects. An effort to simulate and test these effects should be made in future investigations.

The antimicrobial resistance test methods were limited in some ways. Absorbance spectroscopy could be detecting colloid in the urine other than bacteria, for example some of the powdered active materials. Concentration of biofilm (CFU/mL) only quantifies the number of bacteria associated with the biofilms, rather than values associated with the health of the bacteria or the intactness of the extracellular polymeric substance they hide within. Electron or fluorescence microscopy methods are better at quantifying the biofilm inhibition. These methods typically employ the use of fluorescent stains that may help quantify specific damage to the biofilms. Moreover, the use of different strains of bacteria, like *Staphylococcus* and *Pseudomonas*, may lead to different test results because each genus evolved to resist different environmental insults. The composite coatings may also be less effective against more pathogenic species of bacteria, which naturally possess more resistive genes. In addition to bacterial cells, it would also be important to measure the cytotoxicity of the composite films. High concentrations of silver can induce toxicity to human tissues. Testing the coating with human cells or live animals would help determine if the coating is less safe than other silver-type coatings used commercially. Finding the right median between biofilm inhibition and low toxicity to humans is the ultimate goal.

To conclude, catheter associated urinary tract infection is still prevalent in hospitals around the world. Bacteria are the ultimate survivors, able to groom surfaces to their liking and pass on genes that enable resistance to harsh environments. Creating materials that can be used to passively mitigate the transmission of infection is a challenge. The design and analysis of materials that are able to use combined effects to inhibit the attachment and proliferation of bacteria on medical devices is the key to infection control. Although there are active materials shown to have this effect, incorporating them safely onto the surfaces of medical devices is not trivial. Doing so may help save thousands of patients from life threatening infections that cost hospitals billions of dollars to manage.

References

- [1] C. V Gould, C. A. Umscheid, R. K. Agarwal, G. Kuntz, and D. A. Pegues, "Guideline for Prevention of Catheter-Associated Urinary Tract Infection 2009," 2017.
- [2] C. S. Hollenbeak and A. L. Schilling, "The attributable cost of catheter-associated urinary tract infections in the United States : A systematic review," *AJIC Am. J. Infect. Control*, vol. 46, pp. 751–757, 2018.
- [3] P. Singha, J. Locklin, and H. Handa, "A review of the recent advances in antimicrobial coatings for urinary catheters," *Acta Biomater.*, vol. 50, pp. 20–40, 2017.
- [4] J. Tang, Q. Chen, L. Xu, S. Zhang, L. Feng, L. Cheng, H. Xu, Z. Liu, R. Peng, "Graphene Oxide – Silver Nanocomposite As a Highly Effective Antibacterial Agent with Species-Specific Mechanisms," *Appl. Mater. Interfaces*, vol. 5, pp. 3867–3874, 2013.
- [5] Y. Wang, A. Cao, Y. Jiang, X. Zhang, J. Liu, and Y. Liu, "Superior Antibacterial Activity of Zinc Oxide/Graphene Oxide Composites Originating from High Zinc Concentration Localized around Bacteria," *Appl. Mater. Interfaces*, vol. 6, pp. 2791–2798, 2014.
- [6] D. K. Riley, D. C. Classen, L. E. Stevens, and J. P. Burke, "A Large Randomized Clinical Trial of a Silver-Impregnated Urinary Catheter: Lack of Efficacy and Staphylococcal Superinfection," *Am. J. Med.*, vol. 98, no. April, pp. 349–356, 1995.
- [7] S. Sarangapani, "Encrustation and Bacterial Resistant Coatings for Medical Applications," 5,877,243, 1999.
- [8] E. L. Lawrence and I. G. Turner, "Materials for urinary catheters: A review of their history and development in the UK," *Med. Eng. Phys.*, vol. 27, no. 6, pp. 443–453, 2005.
- [9] M. N. Mann, E. R. Fisher, "Perspectives on antibacterial performance of silver nanoparticle-loaded three-dimensional polymeric constructs," *Biointerphases*, vol. 13, no. 6E404, p. 14pp, 2018.
- [10] S. T. Reddy, K. K. Chung, C. J. McDaniel, R. O. Darouiche, J. Landman, and A. B. Brennan, "Micropatterned Surfaces for Reducing the Risk of Catheter-Associated Urinary Tract Infection: An *In Vitro* Study on the Effect of Sharklet Micropatterned Surfaces to Inhibit Bacterial Colonization and Migration of Uropathogenic *Escherichia coli*," *J. Endourol.*, vol. 25, no. 9, pp. 1547–1552, 2011.
- [11] R. M. May, M.G. Hoffman, M.J. Sogo, A.E. Parker, G.A. O'Toole, A.B. Brennan, S.T. Reddy, "Micro-patterned surfaces reduce bacterial colonization and biofilm formation in vitro: Potential for enhancing endotracheal tube designs," *Clin. Transl. Med.*, vol. 3, no. 1, p. 8, 2014.
- [12] R. V. Andino, C. J. Brooks, M. J. Keating, C. F. Morgan, and D. Van Royen, "Apparatus and Methods for Facilitating Wound Healing and Treating Skin," US 2008/0027509 A1, 2008.
- [13] J. B. Skiba, "Current Producing Surface for Treating Biologic Tissue," 7,813,806 B2, 2010.
- [14] H. Wolfmeier, D. Pletzer, S. C. Mansour, and R. E. W. Hancock, "New Perspectives in Biofilm

- Eradication,” *ACS Infect. Dis.*, vol. 4, no. 2, pp. 93–106, 2018.
- [15] J. A. Spadaro, T. J. Berger, S. D. Barranco, S. E. Chapin, and R. O. Becker, “Antibacterial Effects of Silver Electrodes with Weak Direct Current,” *Antimicrob. Agents Chemother.*, vol. 6, no. 5, pp. 637–642, 1974.
- [16] J. L. Del Pozo, M. S. Rouse, J. N. Mandrekar, J. M. Steckelberg, and R. Patel, “The electricidal effect: Reduction of Staphylococcus and Pseudomonas biofilms by prolonged exposure to low-intensity electrical current,” *Antimicrob. Agents Chemother.*, vol. 53, no. 1, pp. 41–45, 2009.
- [17] P. Voegelé, J. Badiola, S.M. Schmidt-Malan, M.J. Karau, K.E. Greenwood-Quaintance, J.N. Mandrekar, R. Patel., “Antibiofilm activity of electrical current in a catheter model,” *Antimicrob. Agents Chemother.*, vol. 60, no. 3, pp. 1476–1480, 2016.
- [18] J. Banerjee, P.D. Ghatak, S. Roy, S. Khanna, C. Hemann, B. Deng, A. Das, J.L. Zweier, D. Wozniak, C.K. Sen, “Silver-Zinc Redox-Coupled electroceutical wound dressing disrupts bacterial biofilm,” *PLoS One*, vol. 10, no. 3, pp. 1–15, 2015.
- [19] J. Banerjee, P.D. Ghatak, S. Roy, S. Khanna, E.K. Sequin, K. Bellman, B.C. Dickinson, P. Suri, V.V. Subramaniam, C.J. Chang, C.K. Sen, “Improvement of human keratinocyte migration by a redox active bioelectric dressing,” *PLoS One*, vol. 9, no. 3, 2014.
- [20] I. E. C. Mott, D. J. Stickler, W. T. Coakley, and T. R. Bott, “The removal of bacterial biofilm from water-filled tubes using axially propagated ultrasound,” *J. Appl. Microbiol.*, vol. 84, pp. 509–514, 1998.
- [21] C. Ergs, L. Bruck, R. R. Rosencrantz, G. Conrads, L. Elling, and A. Pich, “Biofunctionalized Zinc Peroxide Nanoparticles as active oxygen sources and antibacterial agents,” *RSC Adv.*, vol. 7, pp. 38998–39010, 2017.
- [22] A. M. Nandkumar, M. C. Ranjit, S. S. P. Kumar, P. R. Hari, P. Ramesh, and K. Sreenivasan, “Antimicrobial silver oxide incorporated urinary catheters for infection resistance,” *Trends Biomater. Artif. Organs*, vol. 24, no. 3, pp. 156–164, 2010.
- [23] E. Kim, W.H. Kinney, A.R. Ovrutsky, D. Vo, X. Bai, J.R. Honda, G. Marx, E. Peck, L. Lindberg, J.O. Falkinham III, R.M. May, E.D. Chan, “A surface with a biomimetic micropattern reduces colonization of Mycobacterium abscessus,” *FEMS Microbiol. Lett.*, vol. 360, no. 1, pp. 17–22, 2014.
- [24] E. E. Mann, D. Mann, M.R. Mettetal, R.M. May, E.M. Dannemiller, K.K. Chung, A.B. Brennan, S.T. Reddy, “Surface micropattern limits bacterial contamination,” *Antimicrob. Resist. Infect. Control*, vol. 3, no. 1, pp. 1–8, 2014.
- [25] S. Sarica, Y. Akkoc, H. Karapolat, and H. Aktug, “Comparison of the use of conventional, hydrophilic and gel-lubricated catheters with regard to urethral micro trauma, urinary system infection, and patient satisfaction in patients with spinal cord injury: a randomized controlled study,” *Eur. J. Phys. Rehabil. Med.*, vol. 46, no. 4, pp. 473–480, 2010.
- [26] M. Alagiri, “Personal Interview.” University of California San Diego, 2018.
- [27] H. H. Tuson and D. B. Weibel, “Bacteria-surface interactions,” *Soft Matter*, vol. 9, no. 17, pp.

- 4368–4380, 2013.
- [28] L. D. Renner and D. B. Weibel, “Physicochemical Regulation of Biofilm Formation,” *MRS Bull.*, vol. 36, no. 5, pp. 347–355, 2011.
- [29] D. Davies, “Understanding Biofilm Resistance to Antimicrobial Agents,” *Nat. Rev. Drug Discov.*, vol. 2, no. February, pp. 114–122, 2003.
- [30] O. Wahlsten, J. Skiba, I. Makin, and P. Apell, “Electrical field landscape of two electroceuticals,” *J. Electr. Bioimpedance*, vol. 7, no. 1, p. 13, 2016.
- [31] C. Morris, “Bio-electrical stimulation therapy using POSiFECT® RD,” *Wounds UK*, vol. 2, no. 4, pp. 112–115, 2006.
- [32] Z. Li, X. Gu, S. Lou, and Y. Zheng, “The development of binary Mg-Ca alloys for use as biodegradable materials within bone,” *Biomaterials*, vol. 29, no. 10, pp. 1329–1344, 2008.
- [33] C. D. Bernanier, E. B. Feldman, W. P. Flatt, and S. T. St. Jeor, Eds., *Handbook of Nutrition and Food*. Boca Raton: CRC Press, 2002.
- [34] X. Gu, Y. Zheng, Y. Cheng, S. Zhong, and T. Xi, “In vitro corrosion and biocompatibility of binary magnesium alloys,” *Biomaterials*, vol. 30, no. 4, pp. 484–498, 2009.
- [35] W. Chiang, C. Schroll, L. R. Hilbert, P. Møller, and T. Tolker-nielsen, “Silver-Palladium Surfaces Inhibit Biofilm Formation,” *Appl. Environ. Microbiol.*, vol. 75, no. 6, pp. 1674–1678, 2009.
- [36] L. M. Plum, L. Rink, and H. Haase, “The Essential Toxin : Impact of Zinc on Human Health,” *Int. J. Environ. Res. Public Health*, vol. 7, pp. 1342–1365, 2010.
- [37] M. Pourbaix, *Atlas of Electrochemical Equilibria in Aqueous Solutions*, 2nd ed. Houston, Texas, USA: National Association of Corrosion Engineers, 1974.
- [38] J. Sawai, S. Shoji, H. Igarashi, A. Hshimoto, T. Kokugan, M. Shimizu, H. Kojima, “Hydrogen Peroxide as a Antibacterial Factor in Zinc Oxide Powder Slurry,” *J. Ferment. Bioeng.*, vol. 86, no. 5, pp. 521–522, 1998.
- [39] C. E. Bayliss and W. M. Waites, “The Effect of Hydrogen Peroxide and Ultraviolet Irradiation on Non-sporing Bacteria,” *J. Appl. Bacteriol.*, vol. 48, pp. 417–422, 1980.
- [40] D. Goodsell, “Molecule of the Month: Catalase,” *PDB-101*, 2004. [Online]. Available: <http://pdb101.rcsb.org/motm/57>. [Accessed: 17-Feb-2019].
- [41] J. O. Bockris and A. R. Despic, “Electrochemical Reaction,” *Encyclopaedia Britannica*. Encyclopaedia Britannica, inc., 2011.
- [42] J. Rumble, Ed., *CRC Handbook of Chemistry and Physics*, 100th ed. Boca Raton, FL: CRC Press, Taylor & Francis Group, 2019.
- [43] D. A. Skoog and D. M. West, “Introduction to Electroanalytical Chemistry,” in *Principles of Instrumental Analysis*, 1st ed., New York: Holt, Reinhart and Winston, Inc., 1971.

- [44] A. J. Bard and L. R. Faulkner, *Electrochemical Methods: Fundamentals and Applications*, 2nd ed. New York, New York, USA: John Wiley & Sons, 2001.
- [45] Y. Ong, A. Razatos, G. Georgiou, and M. M. Sharma, “Adhesion Forces between E . coli Bacteria and Biomaterial Surfaces,” *Langmuir*, vol. 15, no. 8, pp. 2719–2725, 1999.
- [46] N. Eustathopoulos, M. G. Nicolas, and B. Drevet, Eds., *Wettability at High Temperatures Volume 3, 1*, 1st ed., vol. 3. Oxford: Pergamon Press, 1999.
- [47] L. W. Mckeen, “Plastics Used in Medical Devices,” in *Handbook of Polymer Applications in Medicine and Medical Devices*, Elsevier Inc., 2014, pp. 21–54.
- [48] A. Mata, A. J. Fleischman, and S. Roy, “Characterization of polydimethylsiloxane (PDMS) properties for biomedical micro/nanosystems,” *Biomed. Microdevices*, vol. 7, no. 4, pp. 281–293, 2005.
- [49] S. Berchmans, A. J. Bandodkar, W. Jia, J. Ram, Y. S. Meng, and J. Wang, “An epidermal alkaline rechargeable Ag – Zn printable tattoo battery for wearable electronics †,” *J. Mater. Chem. A*, vol. 2, pp. 15788–15795, 2014.
- [50] R. Vilku, W. J. C. Thio, P. Das Ghatak, C. K. Sen, A. C. Co, and A. Kiourti, “Power Generation for Wearable Electronics: Designing Electrochemical Storage on Fabrics,” *IEEE Access*, vol. 6, pp. 28945–28950, 2018.
- [51] K. Choi, D. B. Ahn, and S. Lee, “Current Status and Challenges in Printed Batteries: Toward Form Factor-Free, Monolithic Integrated Power Sources,” *ACS Energy Lett.*, vol. 3, pp. 220–236, 2018.
- [52] G. A. Ghiurcan, C. Liu, A. Webber, and F. H. Feddrix, “Development and Characterization of a Thick-Film Printed Zinc-Alkaline Battery,” *J. Electrochem. Soc.*, vol. 150, no. 7, pp. 922–927, 2003.
- [53] R. Kumar, J. Shin, L. Yin, J. You, Y. S. Meng, and J. Wang, “All-Printed , Stretchable Zn-Ag 2 O Rechargeable Battery via Hyperelastic Binder for Self-Powering Wearable Electronics,” *Adv. Energy Mater.*, vol. 7, no. 1602096, p. 8pp, 2017.
- [54] K. T. Braam, S. K. Volkman, and V. Subramanian, “Characterization and optimization of a printed , primary silver – zinc battery,” *J. Power Sources*, vol. 199, pp. 367–372, 2012.
- [55] L. Picard, P. Phalip, E. Fleury, and F. Ganachaud, “Chemical adhesion of silicone elastomers on primed metal surfaces: A comprehensive survey of open and patent literatures,” *Prog. Org. Coatings*, vol. 80, pp. 120–141, 2015.
- [56] A. Goyal, A. Kumar, P.K. Patra, S. Mahendra, S. Tabatabaei, P.J.J. Alvarez, G. John, P.M. Ajayan, “In situ Synthesis of Metal Nanoparticle Embedded Free Standing Multifunctional PDMS Films,” *Macromol. Rapid Commun.*, vol. 30, pp. 1116–1122, 2009.
- [57] D. Koh, A. Wang, P. Shneider, B. Bosinski, and K. W. Oh, “Introduction of a Chemical-Free Metal PDMS Thermal Bonding for Fabrication of Flexible Electrode by Metal Transfer onto PDMS,” *Micromachines*, vol. 8, no. 9, p. 280, 2017.
- [58] M. E. Spahr, D. Goers, A. Leone, S. Stallone, and E. Grivei, “Development of carbon conductive

- additives for advanced lithium ion batteries,” *J. Power Sources*, vol. 196, pp. 3404–3413, 2011.
- [59] S. Vadukumpully, J. Paul, N. Mahanta, and S. Valiyaveetil, “Flexible conductive graphene / poly (vinyl chloride) composite thin films with high mechanical strength and thermal stability,” *Carbon N. Y.*, vol. 49, pp. 198–205, 2011.
- [60] J. Clerc, G. Giraud, S. Alexander, and E. Guyon, “Conductivity of a Mixture of Conducting Insulating Grains: Dimensionality Effects,” *Am. Phys. Soc.*, vol. 22, no. 5, pp. 2489–2494, 1980.
- [61] T. Brooks and C. W. Keevil, “A simple artificial urine for the growth of urinary pathogens,” *Lett. Appl. Microbiol.*, vol. 24, pp. 203–206, 1997.
- [62] G. E. F. Lundell and J. I. Hoffman, “The Effect of Light on Silver Chloride in Chemica,” *Bur. Stand. J. Res.*, vol. 4, no. RP 134, pp. 0–5, 1929.